Egyptian Journal of Chemistry

http://ejchem.journals.ekb.eg/

Metal-Organic Frameworks (MOFs) based 2-Amino-1,4-Benzenedicarboxylic Acid linker: Synthesis and Post-Synthetic Modification

Reda M. Abdelhameed [a] ***and Hassan Abdel-Gawad*** [a]*

[a]*Applied Organic Chemistry Department, Chemical Industries Research Institute, National Research Centre, Scopus affiliation ID 60014618, 33 EL Buhouth St., Dokki, Giza 12622, Egypt.*

Abstract

Nanoporous metal-organic frameworks (MOFs) are three-dimensional porous lattices of inorganic-organic linkers. These materials have tunable physiochemical properties such as high porosity, crystalline nature, chemical, thermal and mechanical stability as well. 2-Amino-1,4-benzenedicarboxylic acid plays an important role in metal-organic frameworks synthesis and post-synthetic modification. It reacts with different metals such as: 3d-transition metal (Zn, Co, Cu, Mn, and Fe), 4d-transition metal (Cd, Ag, and Y**)**, s-alkaline metal (Ca**)**, p- metal (Sn and Al) and 4f-lanthanids (Er, La, Dy, Tb, Nd, Yb, Eu, Pr, Gd and Sm**)** to produce MOFs with different structures. The second-biggest application of 2-amino-1,4-benzenedicarboxylic in MOFs is post-synthetic modification because of the presence of the amino group, such as: IRMOF-3, DMOF-1-NH_2, UMCM-1-NH_2, MOF-LIC-1, MIL-53-NH_2, UIO-66-NH_2, MIL-101-NH_2. This functionalized MOFs react with different organic reagents to produce new MOFs with new applications fields such as gas separation, catalysis, gas storage, water treatment, and other different applications.

Keywords: 2-Amino-1,4-Benzenedicarboxylic Acid ; Metal-organic frameworks**;** Synthesis**;** Post-synthetic modification**.**

Abbreviations

BTB=4,4′,4″-benzene-1,3,5-triyl-tribenzoate; BTZ=1*H*-benzotriazole; CSD = Cambridge Structural Database;DABCO=1,4-diazabicyclo[2.2.2]octane; DEF= diethylformamide; DMA=*N*, *N*\-dimethylacetamide; DMA=*N*,*N*'-dimethylacetamide; DMF= dimethylformamide; DMOF=DABCO metal–organic framework; DMSO=dimethyl sulfoxide; DPSI=1,4-dicarboxyphenyl-2-salycilydenimine; ESCP=ethoxysuccinato-cisplatin; IRMOF= Isoreticular metal organic framework; MIL=Materials Institut Lavoisier; MOF=metal organic framework; NH_2BDCH_2=2-amino-1,4-benzenedicarboxylic acid; NMOF=nano metal organic framework; NO=nitric oxide; PXRD=powder X-ray diffraction; SBU=secondary building units; SEM=scanning electron microscope; TEM=transmission electron microscope; UIO=University of Oslo; UMCM=University of Michigan crystalline material; bipy=2, 2'-bipyridine;

---

*Corresponding author e-mail: abdelgawadhassan@hotmail.com.; (Hassan Abdel-Gawad).

Received date 03 January 2022; revised date 12 January 2022; accepted date 12 January 2022

DOI: 10.21608/EJCHEM.2022.114451.5203

bipy-eta= 1,2-bis(4-pyridyl)ethane); bpe=*trans*-1-(2-pyridyl)-2-(4-pyridyl)ethylene; ph=phenyl; phen= 1,10-phenanthroline; py=pyridine.

Table of Contents

1. General introduction

Metal-Organic Frameworks (MOFs) are inorganic–organic solids that may form porous crystalline structures and can be synthesized using a wide range of metal ions and organic ligands.[1] MOFs have numerous potential applications, such as gas storage, [2] gas separations, [3]chemical sensing, [4] ion exchange, [5]drug delivery, [6] removal of heavy metals from aqueous solutions, [7] catalysis [8]and also as photoactive, [9]and luminescent agents.[10]

Several methods are used for the synthesis of metal-organic framework. Solvothermal synthesis is very similar to the hydrothermal route (where the synthesis is conducted in a stainless steel autoclave) the only difference being that the solvent is not water. Microwave synthesis may soon replace conventional solvothermal synthesis based on heat convection. Another method that produces small MOF crystals with decreased reaction times is sonochemical synthesis. While microwave and sonochemical methods decrease MOF synthesis times, they still rely on solvents, whereas mechanochemical synthesis is a solvent-free methodology. In this technique, neat mixtures of linker molecules and metal salts are ground together in a ball mill to produce the desired MOF. [11] One of the most recent developments in the MOFs area is their post-synthetic modification (PSM), which affords new materials with different properties.[12] Post-synthetic methods are important for the following reasons. First, the solvothermal reaction conditions that are used to prepare most MOFs greatly limit the types of functional groups that can be introduced pre-synthetically. Second, MOFs contain an organic ligand component and hence open the possibility of employing the vast range of organic transformations developed by synthetic organic chemists. Finally, because MOFs are highly porous, the ability of reagents to access the interior of the solids suggests that functionalization can be achieved on both the interior and exterior of the material.[13] One of the linkers most used to build up porous MOFs structures is 2-amino-1,4-benzenedicarboxylic acid (NH_2BDCH_2). This review highlights some important functional metal–organic framework materials having the NH_2BDCH_2 as the backbone linker such as: IRMOF-3, DMOF-1-NH_2, UMCM-1-NH_2, MOF-LIC-1, MIL-53-NH_2, UIO-66-NH_2 and MIL-101-NH_2. This review is intended to provide the reader with a comprehensive overview of the considerations associated with synthesis and post-synthetic modification of metal□organic frameworks containing 2-amino-1,4-benzenedicarboxylic acid. Herein we attempt to capture the complete history of MOFs synthesis with 2-amino-1,4-benzenedicarboxylic acid and PSM to date, as well as described in the most recent reports in the Cambridge Structural Database (CSD).

2. Synthesis of MOFs using 2-amino-1,4-benzenedicarboxylic acid as synthon

2.1. 3d-transition metal-MOFs [Zn, Co, Cu, Mn, Fe]

2.1.1. Zn-MOF

In 2001 Yaghi *et al.*, [14] demonstrated that the pores of MOFs can be functionalized with potentially reactive groups ($-NH_2$) without changing the secondary building units (SBU) or the underlying framework topology. They synthesized $Zn(NH_2BDC)(DMF)\cdot(PhCl)_{0.25}$ (MOF-46) (Figure 1A) by slow diffusion of a mixture containing chlorobenzene–trimethylamine into DMF–chlorobenzene solvent mixture containing $Zn(NO_3)_2\cdot6H_2O$ and H_2NBDCH_2 at room temperature for 4–7 days. This compound was characterized by elemental microanalysis and single crystal X-ray diffraction. In 2002, a new class of porous materials {cubic gold crystals: $Zn_4O(NH_2BDC)$ 3.7DEF (Figure 1B)} was constructed from octahedral Zn-O-C clusters and NH_2BDCH_2 as the linker. This MOF differs from the above one in the synthetic method and its structure. This material was used in methane storage.[15] In 2006, the reaction of $Zn(NO_3)_24H_2O$ with NH_2BDCH_2 in presence of DEF yielded $[Zn_4(NH_2BDC)_3(NO_3)_2(H_2O)_2]$ (Figure 1C). [16] This structure is composed by trigonal clusters, in which two zinc atoms are bridged by the carboxylate functionalities of three NH_2BDC linkers. The remaining coordination site of each zinc atom is occupied by either a nitrate anion or a water molecule to maintain the charge neutrality of the structure. This MOF has properties for gas storage and catalysis applications. In 2007, the photoluminescent coordination compound $[Zn_2(NH_2BDC)_2(bipy)_2(H_2O)_2]$ (Figure 2A) was synthesized by reaction of 2-amino-1,4-benzenedicarboxylic acid and the *N*-containing ligand 2,2'-bipyridine with $Zn(NO_3)_2.4H_2O$ in the presence of NaOH. [17]

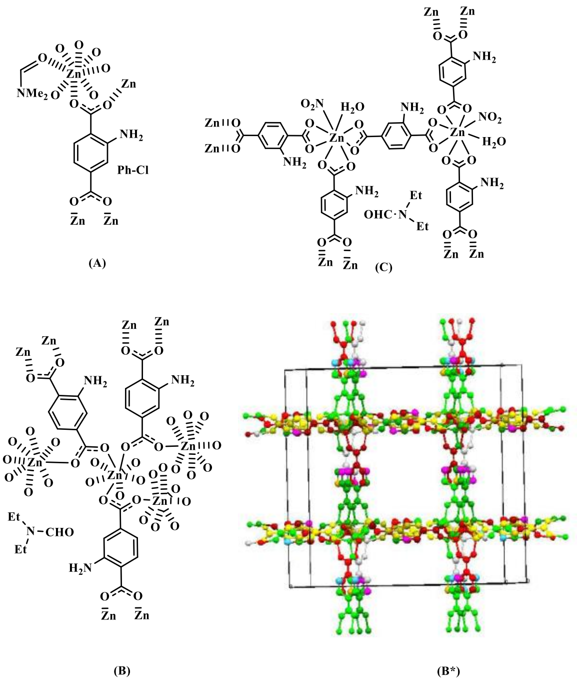

Fig. 1. Local environment of the organic linkers in A) MOF-46, B) MOF-5, C) $[Zn_4(NH_2BDC)_3(NO_3)_2(H_2O)_2]$. (B*) crystal structure of MOF-5, red is oxygen atom; pink is nitrogen atom; green is carbon atom; yellow is zinc atom

This material exhibits green photoluminescence in the solid state at room temperature. In the above approaches, many of these MOFs have 2D structures. In 2008, yellow block crystals of $\{[Zn_3(NH_2BDC)_3(H_2O)_2].5DMF\}$ (Figure 2B) were synthesized by reaction of $Zn(NO_3)_2.6H_2O$ with H_2NBDCH_2 in DMF/H_2O. Single crystal X-ray analysis shows that $\{[Zn_3(NH_2BDC)_3(H_2O)_2].5DMF\}$ is a 3-D MOF composed of the SBUs of $Zn_3(COO)_6$. [18] This compound has a reasonably large Langmuir surface area, while a larger surface area may be obtained with a higher activating temperature. Also in 2008, brown crystals of $[Zn(NH_2BDC)(H_2O)_2]$ (Figure 2C) were prepared by addition of imidazole, $Zn(NO_3)_2.6H_2O$ and 2-amino-1,4-benzenedicarboxylic acid in a mixture of methanol/water. [19] These compounds exhibit blue photoluminescence and may be good candidates for photoactive materials.

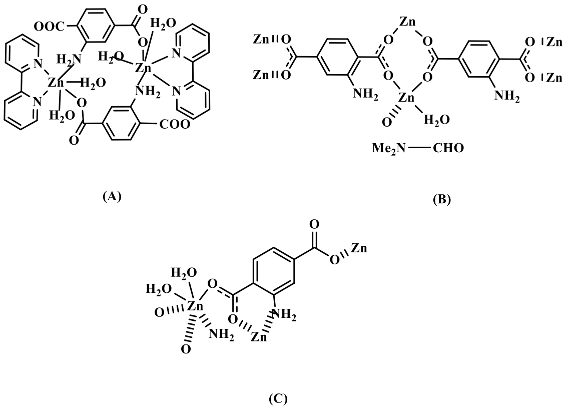

Fig. 2. Local environment of the organic linkers in A) $[Zn_2(NH_2BDC)_2(bipy)_2(H_2O)_2]$, B) $[Zn_3(NH_2BDC)_3(H_2O)_2].5DMF$, C) $[Zn(NH_2BDC)(H_2O)_2]$

In 2009, 2-amino-1,4-benzenedicarboxylic acid was found to be a suitable building block for the construction of two MOFs having isoreticular structures, DMOF-1-NH_2 and UMCM-1-NH_2.[20] The former (Figure 3) was prepared by mixing NH_2-$BDCH_2$, $Zn(NO_3)_2.4H_2O$ and DABCO (1,4-diazabicyclo[2.2.2]octane) in the presence of DMF. UMCM-1-NH_2 is a highly porous MOF and consists of both NH_2-BDC and 4,4′,4″-benzene-1,3,5-triyl-tribenzoate (BTB) (Figure 3C) linkers with Zn_4O as SBUs. UMCM-1-NH_2 was synthesised by addition of $Zn(NO_3)_2{\cdot}4H_2O$, 2-amino-1,4-benzenedicarboxylic acid and 4,4′,4″-benzene-1,3,5-triyl-tribenzoic acid in presence of DMF at 85 °C/48 h. Also in 2009, Xu and Yang [21]synthesised a new binuclear complex (yellow crystal) $\{[Zn(NH_2BDC)(H_2O)]{\cdot}3(DMSO){\cdot}H_2O\}$ (Figure 4A), prepared with $Zn(NO_3)_2{\cdot}6H_2O$ and 2-amino-1,4-benzenedicarboxylic acid in a DMSO solution. The crystal structure was confirmed by elemental analysis and single crystal X-ray diffraction. Single-crystal X-ray diffraction reveals that the Zn^{2+} is five-coordinated. In the above approaches, it is not easy to identify metal ions with which the intended framework geometry can be generated, or to establish the exact chemical conditions for the in situ formation of specific SBUs. This uncertainty arises from the existence of various coordination numbers for a given metal.

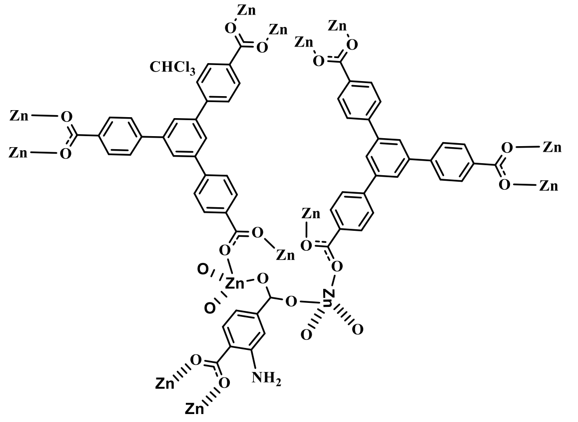

Fig. 3. Local environment of the organic linkers in UMCM-1-NH_2

To overcome these difficulties, the microporous interpenetrated framework $\{[Zn_5(BTZ)_6(NH_2BDC)_2(H_2O)_2].7DMA\}$, (BTZ = 1*H*-benzotriazole, DMA = *N,N*'-dimethylacetamide) (Figure 4B) was produced by using a predesigned tetrahedral metal cluster and a linear organic ligand.[22] In 2010, Kim *et al.* [23]studied the crystal structure of an ordered IRMOF-3 (α-IRMOF-3) (Figure 4C). This compound was an example of polymorphism due to the formula $[Zn_4O(H_2N\text{-}BDC)_3]$, SBUs and connectivity patterns were nearly the same as the known IRMOF-3.

In 2011, $[Zn(NH_2BDC)(py)_2]_n$ was prepared by mixing 2-aminobenzene-1,4-dicarboxylic acid, pyridine and Zn^{2+} cations . [24]All the pyridine (py) rings and all the amino groups point away from the helix to generate a hollow tube with a cross-section of approximately 8 × 8 Å running parallel to the crystallographic c direction. Each single-stranded helix is interdigitated with four neighbouring helices via N-H···O hydrogen bonds, which gives rise to a dense homochiral three-dimensional supramolecular network (Figure 4D).

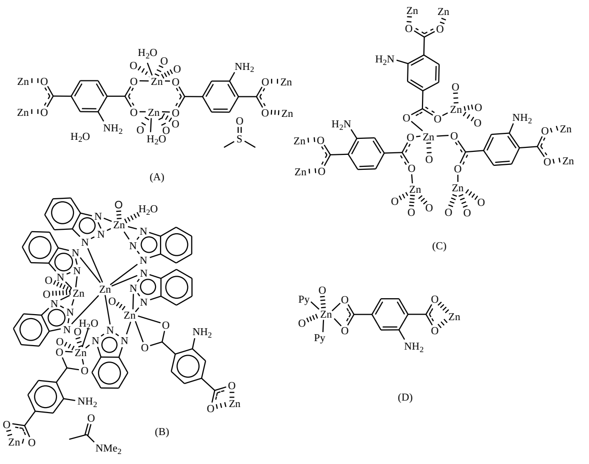

Fig. 4. Local environment of the organic linkers in A) $\{[Zn(NH_2BDC)(H_2O)]\cdot 3DMSO)\cdot H_2O\}n$,B)$\{[Zn_5(BTZ)_6(NH_2BDC)_2(H_2O)_2]$. 7DMA}, C) α-IRMOF-3, D) $[Zn(NH_2BDC)(py)_2]_n$

2.1.2. *Co-MOF*

[Co{1,2-bis(4-pyridyl)ethane}(NH_2BDC)] red block crystals were synthesised by reaction of 2-aminobenzene-1,4-dicarboxylic acid with 1,2-bis(4-pyridyl)ethane and cobalt nitrate in a 1:1:1 ratio. This compound displays a fivefold diamond-type net. The *O*-donor ligands adopt different coordination modes forming different kinds of building blocks, which finally aggregate to generate different supra molecular architectures, due to the influence of the substituent groups. The amino group in 2-aminobenzene-1,4-dicarboxylic acid plays an important role in affecting the coordination mode of the carboxylate group. This compound (Figure 5) has photoluminescence properties. [25]

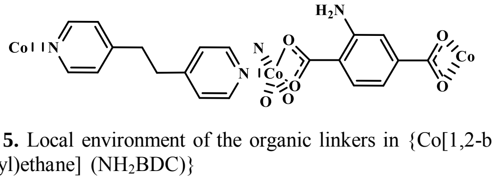

Fig. 5. Local environment of the organic linkers in {Co[1,2-bis(4-pyridyl)ethane] (NH_2BDC)}

2.1.3. *Cu-MOF*

Green crystals of $Cu(H_2O)(phen)(NH_2BDC)\cdot(DMF)$ (Figure 6A) was synthesized by mixing solutions of $Cu(ClO_4)_2.6H_2O$, 2-aminobenzene-1,4-dicarboxylic acid and 1,10-phenanthroline in DMF. [26]$CuCl_2$ reacts with 1,4-dicarboxyphenyl-2-salycilydenimine (DPSI) in presence of methanol to produce green block shaped crystals $[Cu_2(DPSI)_2(NH_2BDC)(H_2O)(MeOH)].4H_2O$ (octahedral geometry) (Figure 6B). In fact, structural analysis shows a bimetallic species with two DPSI ligands, two copper-coordinated solvent molecules, and also a N-coordinated 2-amino-1,4-benzenedicarboxylic acid. Phenylsalicylidenimine ligands are attractive because of the contemporary presence of the aromatic pi conjugated systems and functional H donor and H acceptor groups, giving functional materials. [27]

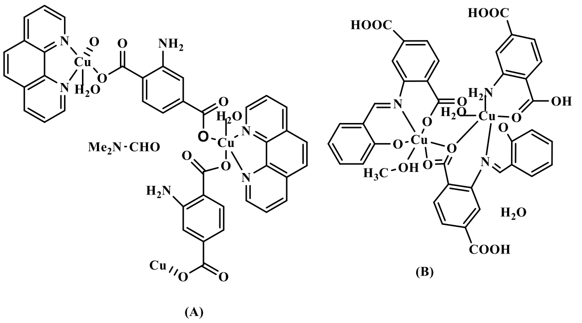

Fig. 6. Local environment of the organic linkers in A) $Cu(H_2O)(phen)(NH_2BDC)\cdot(DMF)$,B)$[Cu_2(DPSI)_2(NH_2BDC)(H_2O)(MeOH)].4H_2O$

2.1.4 *Mn-MOF*

Light brown crystals of $[28]_n$ CPO-10 (Figure 7A) have been synthesized by solvothermal methods, using $MnCl_2.4H_2O$, 2-amino-1,4-benzenedicarboxylic acid, tetrahydrofuran and diethylformamide. CPO-10 is based on linear trinuclear building units of carboxylato-bridged octahedral Mn(II) ions that are cross linked by the 2-amino-1,4-benzenedicarboxylic ligands into a 3D structure. This compound has 1D channels that contain solvent molecules and the magnetic measurements indicate antiferromagnetic couplings between the Mn^{2+} ions. [28] $[Mn(NH_2BDC)(bipy\text{-}eta)_{0.5}]_n$ (bipy-eta= 1,2-bis(4-pyridyl)ethane) (Figure 7B) was prepared by reaction of the Mn^{2+} ion with bipy-eta and 2-amino-1,4-benzenedicarboxylic acid .

This compound was characterized by IR spectroscopy, elemental analysis, and single-crystal X-ray diffraction. [29] Brown block crystals of $[Mn(H_2O)_2(NH_2BDC)]_n$, (Figure 6C) possess a hydrogen-bonded 3D network. Single crystal X-ray analysis show that the Mn^{2+} ions are connected with l2-carboxylates to form left handed and right handed chiral helix chains $(–Mn–O–C–O–)_n$. [30] Manganese (II) nitrate reacts with two dicarboxylic acid ligands, 2-amino-1,4-benzenedicarboxylic acid and 1,4-benzenedicarboxylic acid (H_2BDC) in DMF to give $[Mn_3(NH_2BDC)_3(DMF)_2]$ (Figure 7D). This MOF was used in Lewis catalysis for the cyanosilylation of acetaldehyde and re-used without any loss of activity. [31]

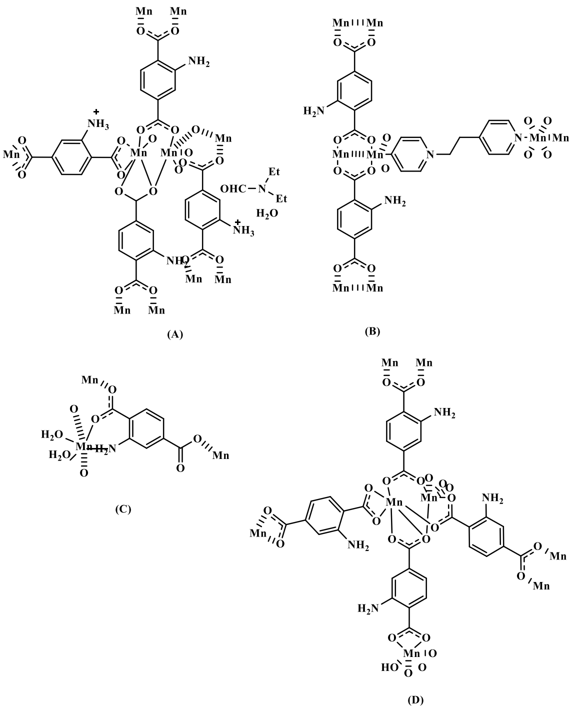

Fig. 7. Local environment of the organic linkers in A){$[Mn_3(NH_2BDCH)_2(NH_2BDC)_2](H_2O)_2(DEF)_4$} structure and B) the structure of $[Mn(NH_2BDC)(bipy\text{-}eta)_{0.5}]_n$ in its pure form, C) $[Mn(H_2O)_2(NH_2BDC)]_n$, D) $[Mn_3(NH_2BDC)_3(DMF)_2]$

2.1.5 *Fe-MOF*

The 3D framework material Fe-MIL101-NH_2 (Figure 8), was synthesized by solvothermal reaction of $FeCl_3$ and 2-amino-1,4-benzenedicarboxylic acid in protic as well as aprotic reaction media. The material was characterized using X-ray diffraction, IR spectroscopy; and thermogravimetric, elemental, and energy dispersive X-ray analysis. [32]

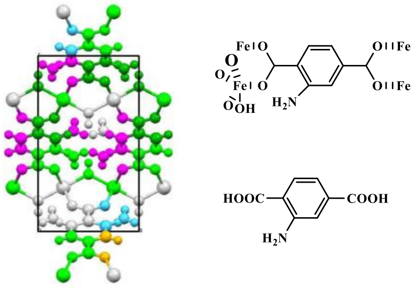

Fig. 8. Local environment of the organic linkers in Fe-MIL101-NH_2 (right), crystal structure of Fe-MIL101-NH_2 (left)

2.2. 4d-transition metal-MOFs [Cd, Ag, Y]

2.2.1 *Cd-MOF*

$[Cd(NH_2BDC)phen(H_2O)]\cdot H_2O$, (phen = 1,10-phenanthroline) (Figure 9A) is the first structurally characterized Cd^{2+} complex with the 2-amino-1,4-benzenedicarboxylic ligand. It was prepared by reaction of 2-amino-1,4-benzenedicarboxylic acid and N-containing ligand 1,10-phenanthroline with $Cd(NO_3)_2\cdot 4H_2O$ in the presence of NaOH. X-ray crystallographic studies show that this compound contains chains and a 3D supramolecular network via inter chain hydrogen bonds and pi–pi stacking interactions.

Green photoluminescence can be observed for this compound in the solid state at room temperature.[17] Yellow hexagonal crystals [18] $(Me_2NH_2)_2[Cd_3(NH_2BDC)_4]\cdot 2DMF\cdot 2.5H_2O$ (Figure 9B) was synthesized by addition of $Cd(NO_3)_2\cdot 6H_2O$ with NH_2BDCH_2 in DMF/H_2O.

Single crystal X-ray analysis shows that this is a 3-D MOF composed of the SBUs of $Cd_3(COO)_8$ and there are non-removable guest $Me_2NH_2^+$ cations clogged in the channels.

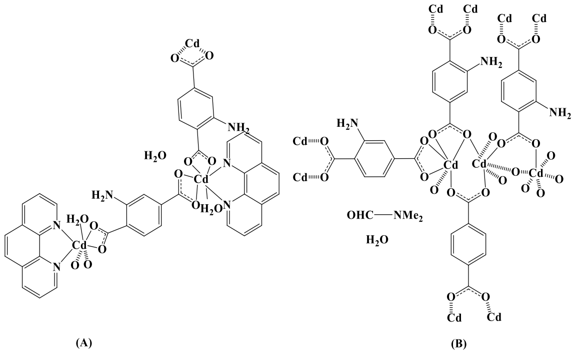

Fig. 9. Local environment of the organic linkers in A) $[Cd(NH_2BDC)phen(H_2O)]\cdot H_2O$,B)$(Me_2NH_2)_2[Cd_3(NH_2BDC)_4]\cdot 2DMF.2.5H_2O$

Colorless crystals of $[Cd(NH_2BDC)(H_2O)_2]\cdot 2H_2O$ (Figure 10A) were prepared by nicotinamide, $Cd(NO_3)_2\cdot 4H_2O$, 2-amino-1,4-benzenedicarboxylic acid in presence of water and methanol. This material has a three-dimensional supramolecular network and exhibits blue photoluminescence. X-ray crystallography prove that the amino group of the 2-amino-1,4-benzenedicarboxylate coordinates to the metal(II) ions. [19] The 3D porous $[Me_2NH_2]_2[Cd_2(NH_2BDC)_3]\cdot 4DMA$ (Figure 10B) (DMA=N,N\-dimethylacetamide) has been solvothermally synthesized with a dimethylammonium template by adding $Cd(NO_3)_2\cdot 4H_2O$ to NH_2BDCH_2 in the presence of N,N\-dimethylacetamide. [33]The results show that the dimethylammonium template can be successfully employed to access new types of structures that otherwise are not obtainable, including a chiral framework, a distorted MOF-5-like framework, low-symmetry SBUs, two types of helical nanotube-like channels, and permanent porosity. Solvothermal reaction of $Cd(NO_3)_2\cdot 4H_2O$, 4,4′-bipyridine (bpy), and 2-amino-1,4-benzenedicarboxylic acid in DMF yielded $Cd(NH_2BDC)(bpy)$ (Figure 10C). This compound has potential as a luminescent probe. In addition, the available amino groups and hierarchical pores in these MOF make it good for post-synthetic covalent modification for further applications. [34]

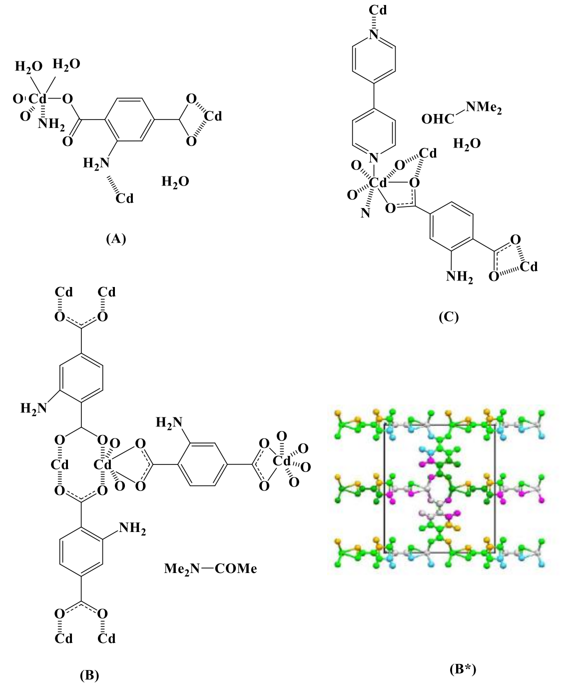

Fig. 10. Local environment of the organic linkers in A) $[Cd(NH_2BDC)(H_2O)_2]\cdot 2H_2O$,B)$[Me_2NH_2]_2[Cd_2(NH_2BDC)_3]\cdot 4DMA$, C) $Cd(NH_2BDC)(bpy)$; (B*) crystal stucture of B, red is oxygen atom; pink is nitrogen atom; green is carbon atom; yellow is zinc atom

2.2.2 *Ag-MOF*

Yellow block crystals of $[Ag(NH_2BDC)_{1/2}(bpe)]_n$ (Figure 11) were synthesised by mixing the 2,4\-bipyridyl linker *trans*-1-(2-pyridyl)-2-(4-pyridyl)ethylene (bpe), 2-amino-1,4-benzenedicarboxylic acid and $AgNO_3$ in methanol/water. The presence of an amino group of 2-amino-1,4-benzenedicarboxylic acid leads to the formation of additional H-bonding interactions. This material was shown to be strongly fluorescent emission at room temperature. [35]

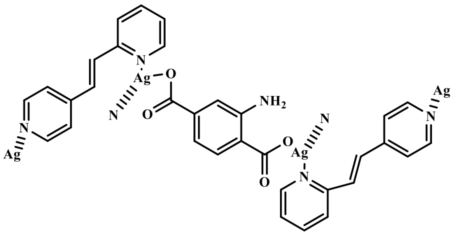

Fig. 11. Local environment of the organic linkers in $[Ag(NH_2BDC)_{1/2}(bpe)]_n$

2.2.3 *Y-MOF*

$[Y_2(NH_2BDC)_3(DMF)_4]_n$ (Figure 12) contains one Y^{3+} ion, three half-molecules of the 2-amino-1,4-benzenedicarboxylate and two *O*-bonded DMF molecules. [36]

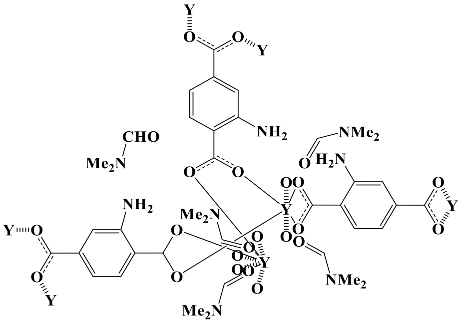

Fig. 12. Local environment of the organic linkers in $[Y_2(NH_2BDC)_3(DMF)_4]_n$

2.3. s-alkaline-earth metal-MOFs [Ca]

2.3 *Ca-MOF*

Colorless crystals of $[Ca(NH_2BDC)(DMF)]$ (Figure 13) were synthesized from $Ca(NO_3)_2 \cdot 4H_2O$ and 2-amino-1,4-benzenedicarboxylic acid by solvothermal reactions and microwave-assisted solvothermal reactions. Single crystal X-ray diffraction shows that the structure consists of an extended 3D framework and inorganic SBUs are connected through the polycarboxylate ligands to form 3D channel structures.[37]

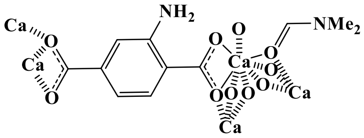

Fig. 13. Local environment of the organic linkers in $[Ca(NH_2BDC)(DMF)]$

2.4. p- metal-MOFs [Sn, Al]

2.4. 1 *Sn-MOF*

Tin-organic framework $[Sn_2(ph)_6(NH_2BDC)]$ (Figure 14) contains two triphenyl tin groups bridged by a 2-amino-1,4-benzenedicarboxylate ligand. This compound has potential properties in antitumor and cancer chemotherapy. [38]

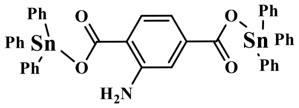

Fig. 14. Local environment of the organic linkers in $[Sn_2(ph)_6(NH_2BDC)]$

2.4.2 *Al-MOF*

$AlCl_3 \cdot 6H_2O$ react with 2-amino-1,4-benzenedicarboxylic acid in the presence of water/methanol as solvent, and led to the formation of new 12-connected, highly porous, and stable metal–organic framework $\{[Al_4(OH)_2(OCH_3)_4(NH_2BDC)_3] \cdot xH_2O\}$ Al-MIL-53-NH_2 (Figure 15). [39]Al-MIL-53-NH_2 was shown to be a stable, highly active, basic catalyst in a Knoevenagel condensation, and to be well-suited for CO_2/CH_4 separation.[40, 41]

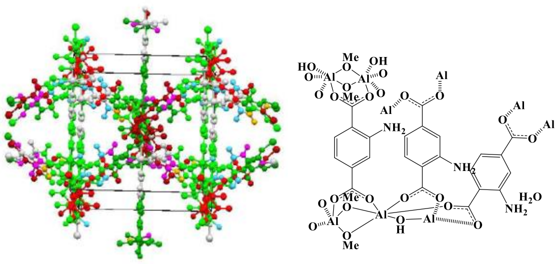

Fig. 15. Local environment of the organic linkers in Al-MIL-53-NH_2 (right); crystal structure of Al-MIL-53-NH_2 (left), red is oxygen atom; pink is nitrogen atom; green is carbon atom; yellow is zinc atom

2.5. 4f-lanthanids-MOFs [Er, La, Dy, Tb, Nd, Yb, Eu, Pr, Gd, Sm]

2.5.1 *Er-MOF*

The brown lamella crystals of $Er_2(NH_2BDC)_3 \cdot 5.5H_2O$ (Figure 16A) were prepared by reaction of 2-amino-1,4-benzenedicarboxylic acid with $Er(NO_3)_3$ at 140 ºC for 48 hour. [42]It is stable in air and insoluble in common solvents. Crystallographically shows that one erbium atom is coordinated by 8 oxgyen atoms, six from five carboxylic group of 2-amino-1,4-benzenedicarboxylic ligand and two from water molecules. $[Er_2(NH_2BDC)_3(phen)_2(H_2O)]_n$ (Figure 16B) was prepared by hydrothermal reaction.

The compound is very stable in air at ambient temperature and insoluble in common solvents such as water, alcohol and acetone.[43]

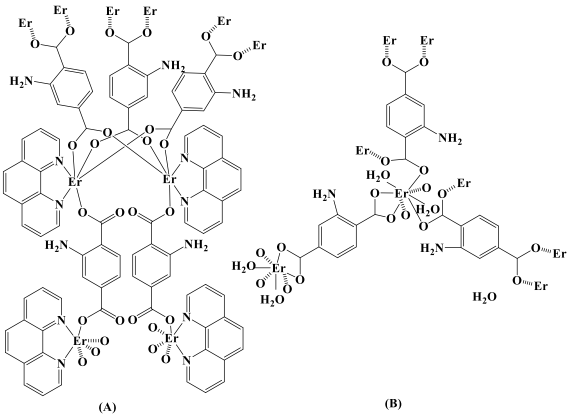

Fig. 16. Local environment of the organic linkers in A) of $Er_2(NH_2BDC)_3.5.5H_2O$,B)$[Er_2(NH_2BDC)_3(phen)_2(H_2O)]_n$

2.5.2 *La-MOF*

$[La_2(NH_2BDC)_3{\cdot}(H_2O)_5](H_2O)_2$ (Figure 17A) was prepared by hydrothermal. The carboxyl groups of 2-amino-1,4-benzenedicarboxylic acid link La^{3+} ion centers producing one-dimension channels.[44] $[La(NH_2BDC)_{1.5}(phen)(H_2O)]_n$ (Figure 17B) was prepared by hydrothermal reaction.

This material is stable in air at ambient temperature and insoluble in water, alcohol and acetone.[45]

2.5.2 *Dy-MOF*

A mixture of 2-amino-1,4-benzenedicarboxylic acid, NaOH, distillated water , $Dy(NO_3)_3$ at 150 °C for 72 h give crystals $[Dy(NH_2BDC)_{1.5}{\cdot}(H_2O)_2]{\cdot}(H_2O)_2$ (Figure 18A).

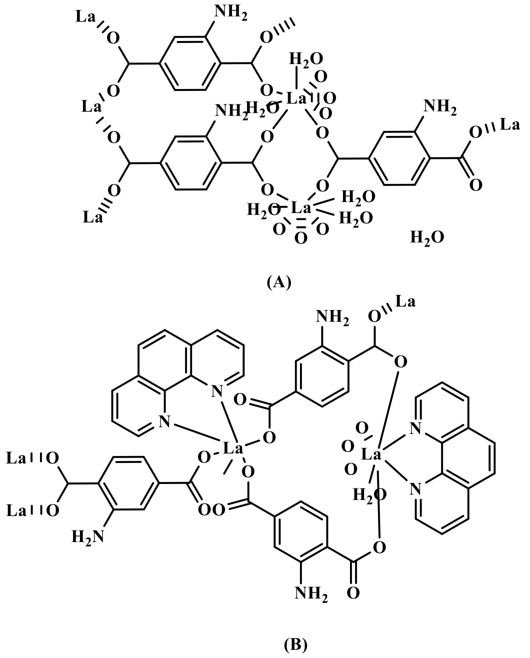

Fig. 17. Local environment of the organic linkers in A) $[La_2(NH_2BDC)_3{\cdot}(H_2O)_5](H_2O)_2$, B) $[La(NH_2BDC)_{1.5}(phen)(H_2O)]_n$

The material is stable in air and insoluble in water and organic solvents. It consists of an open-framework in which the Dy^{3+} ion center occupies a distorted square anti-prism coordination site. Both carboxyl groups of each ligand bind to ion centers in the same coordination fashion to furnish channel-structures.

It is of importance to observe coordination waters and amino groups dangling in the channels and guest waters within channels joining these pendant groups via hydrogen bonds. These channels are hydrophilic. [45] $\{[Dy_2(NH_2BDC)_3(DMF)_4]{\cdot}2DMF\}_\infty$ (Figure 18B) have cubic topology and were synthesized using solvothermal conditions.[46]

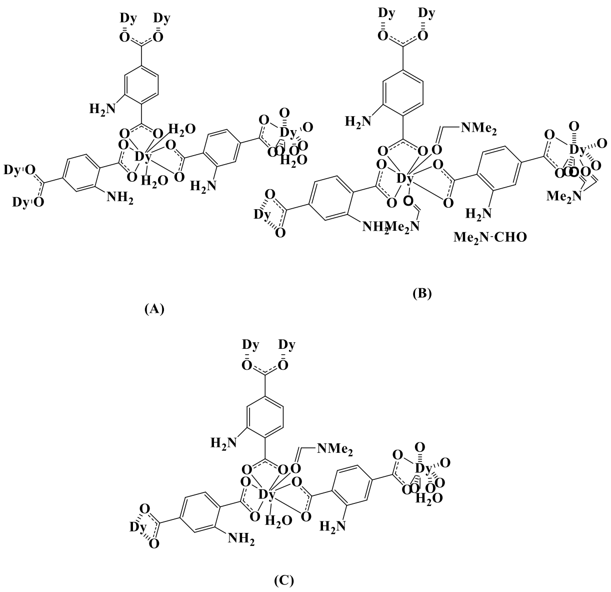

Fig. 18. Local environment of the organic linkers in A)$[Dy(NH_2BDC)_{1.5}\cdot(H_2O)_2]\cdot(H_2O)_2$,B)$\{[Dy_2(NH_2BDC)_3(DMF)_4]\cdot2DMF\}_\infty$,C)$Dy_2(NH_2BDC)_3(DMF)_2(H_2O)_2$

$Dy_2(NH_2BDC)_3(DMF)_2(H_2O)_2$ (Figure 18C) has luminescent properties. It was prepared by reaction of $Dy(NO_3)_3$ with 2-amino-1,4-benzenedicarboxylic acid (2:3 ratio) in presence of DMF and H_2O and their crystal structures determined by X-ray crystallography.[43]Single-crystal X-ray analyses show that each Dy atom is nine-coordinated, surrounded by one DMF and one water molecule.

2.5.3 *Tb-MOF*

$[Tb(NH_2BDC)_{1.5}(H_2O)_2]\cdot2H_2O$ (Figure 19A) was obtained by the hydrothermal synthesis. The carboxyl groups link Tb^{3+} via the chelating or bridging bond construct one-dimension channels in which pendant functional groups can further connect with guest water molecules in channels through hydrogen bond.[47]$[Tb_2(NH_2BDC)_3(phen)_2(H_2O)]_n$ (Figure 19B) was prepared by hydrothermal reactions. It is stable in air at ambient temperature and almost insoluble in common solvents such as water, alcohol and acetone.[48] $\{[Tb_2(NH_2BDC)_3(DMF)_4]\cdot2DMF\}_\infty$ (Figure 19C) with cubic topology have been synthesized using solvothermal conditions. The networks were generated via formation of a dinuclear Tb secondary building block, involving the dicarboxylate ligand as a bridge. The luminescent properties of the Tb^{3+} complexes showed characteristic emissions at room temperature.[46]

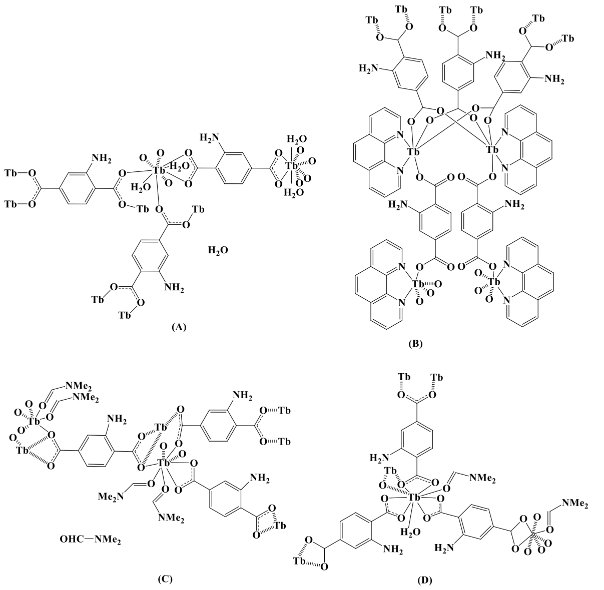

Fig. 19. Local environment of the organic linkers in A) $[Tb(NH_2BDC)_{1.5}(H_2O)_2]\cdot2H_2O$, B) $[Tb_2(NH_2BDC)_3(phen)_2(H_2O)]_n$ C)$\{[Tb_2(NH_2BDC)_3(DMF)_4]\cdot2DMF\}_\infty$,D)$Tb_2(NH_2BDC)_3(DMF)_2(H_2O)_2$

$Tb_2(NH_2BDC)_3(DMF)_2(H_2O)_2$ (Figure 19D) was prepared by addition of $Tb(NO_3)_3$ to 2-amino-1,4-benzenedicarboxylic acid (2:3 ratio) in presence of DMF and H_2O and their crystal structures determined by X-ray crystallography. Each Tb atom is nine-coordinated, surrounded by one DMF and one water molecule. This product has luminescent properties.[43]

2.5.4 *Nd-MOF*

The clear-brown crystal $[Nd(NH_2BDC)_{1.5}(H_2O)_2]\cdot2H_2O$ (Figure 20A) is stable in air and insoluble in common solvents. It has a microporous structure and is prepared by addition of 2-amino-1,4-benzenedicarboxylic acid, NaOH, distilled water and $Nd(NO_3)_3$ at 146 °C for 48 h. The amino groups do not coordinate with metal ions; these groups play an important role in creation of hydrogen bonds.[49]

Microporous $\{[Nd_3(NH_2BDC)_3(NH_3BDC)_3]\cdot 9H_2O\}_n$ (Figure 20B) [50] is stable in air and insoluble in water and common organic solvents. It was synthesized by slow diffusion of aqueous solution of NH_2BDCH_2 and $Nd(NO_3)_3\cdot 6H_2O$ in 2-propanol. This MOF crystallizes in the cubic space group *Ia*-3, composed of the secondary building blocks of trinuclear lanthanide cores as six-connecting nodes, which are enclosed by twelve NH_2BDC bridges. The bridging of the Ln_3 SBUs forms a NaCl-type crystal lattice containing cavities occupied by guest molecules. The results show that this is the first observation of the assembly of the linear trinuclear lanthanide clusters into a microporous framework. Thermal gravimetry and powder X-ray diffraction analyses show that the large cavity can accommodate other small molecules such as methanol after removal of the guest water molecules. Most importantly, the host structure remains intact during the course. The 2-amino-1,4-benzenedicarboxylic ligand, as a good spacer, can be exploited to create novel lanthanide-containing materials providing microporous structures. The large size of the cavities offers appreciable potential for the guest molecule occupation and investigation in this direction is in progress.

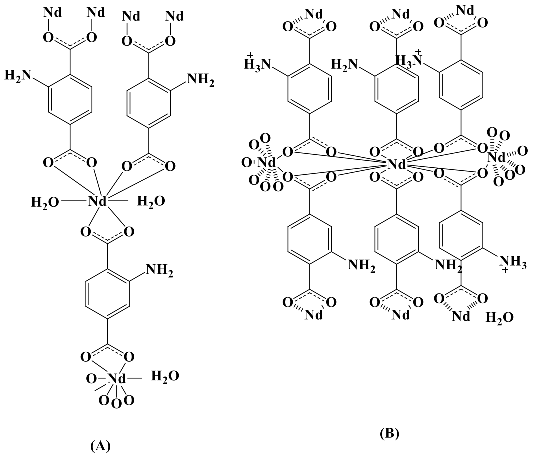

Fig. 20. Local environment of the organic linkers in A) $[Nd(NH_2BDC)_{1.5}(H_2O)_2]\cdot 2H_2O$,B)$\{[Nd_3(NH_2BDC)_3(NH_3BDC)_3]\cdot 9H_2O\}_n$

New potentially porous lanthanide containing molecular open frameworks with general chemical formula $[Nd(NH_2BDC)(NH_3BDC), nH_2O]_\infty$ (Figure 21A), $8 < n < 11$ were synthesised from 2-amino-1,4-benzenedicarboxylic acid and hydrated lanthanide chloride. These compounds crystallize in the cubic system. The crystal structure can be described as the juxtaposition of large channels with square cross-section. The channels are filled by highly disordered crystallization water molecules. The dehydration of the compounds by freeze-drying is possible and most of the crystallization water molecules can be removed without destruction of the molecular skeleton. [43]

$Nd_2(NH_2BDC)_3(DMF)_2(H_2O)_2$ (Figure 21B) was prepared by heating $Nd(NO_3)_3$ and 2-amino-1,4-benzenedicarboxylic acid in a 2:3 ratio in mixed DMF/H_2O solution at 80 °C and their crystal structures determined by X-ray crystallography.[43] Single-crystal X-ray analyses shows that this compound has 3D frameworks and each Nd atom is nine-coordinated, surrounded by one DMF and one water molecule, and it has luminescent properties.

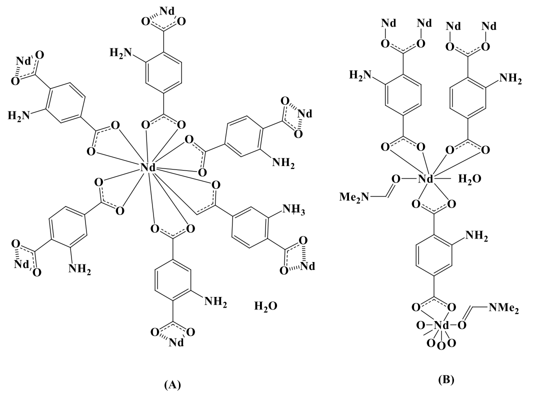

Fig. 21. Local environment of the organic linkers in A) $[Nd(NH_2BDC)(NH_3BDC),nH_2O]_\infty$,B)$Nd_2(NH_2BDC)_3(DMF)_2(H_2O)_2$

2.5.5*Yb-MOF*

$[Yb_2(OH)(NH_2BDC)_{2.5}(phen)_2]_n\cdot 1.75H_2O$ (Figure 22) was prepared by hydrothermal reaction. It is very stable in air at ambient temperature and insoluble in common solvents such as water, alcohol and acetone.[48]

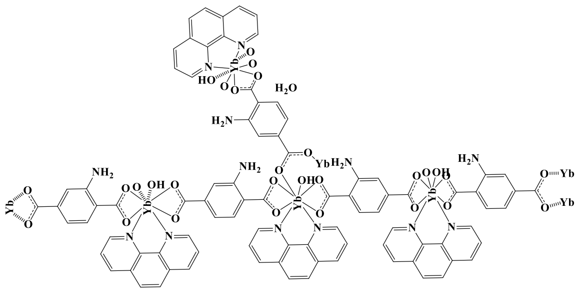

Fig. 22. Local environment of the organic linkers in $[Yb_2(OH)(NH_2BDC)_{2.5}(phen)_2]_n\cdot1.75H_2O$

2.5.6 *Eu-MOF*

$[Eu(NH_2BDC)_{1.5}(phen)(H_2O)]_n$ (Figure 23A) was prepared by hydrothermal reaction. It is stable in air and insoluble in solvents such as water, alcohol and acetone.[48] New lanthanide 2-amino-1,4-benzenedicarboxylate coordination polymers $[Eu(NH_2BDC)_{1.5}(H_2O)_2]\cdot2H_2O$ (Figure 23B) was obtained by hydrothermal synthesis. The carboxyl groups link Eu^{3+} via the chelating or bridging bond construct one-dimension channels in which pendant function groups can further connect with guest water molecules in channels through hydrogen bond. [47]

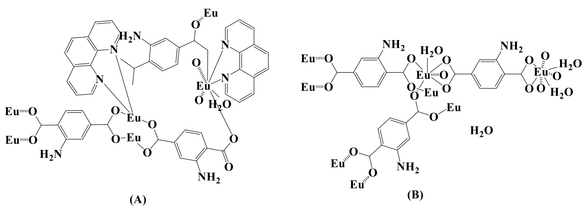

Fig. 23. Local environment of the organic linkers in A) $[Eu(NH_2BDC)_{1.5}(phen)(H_2O)]_n$, B) $[Eu(NH_2BDC)_{1.5}(H_2O)_2]\cdot2H_2O$

$\{[Eu_2(NH_2BDC)_3(DMF)_4]\cdot2DMF\}_\infty$ (Figure 24A) with cubic topology have been synthesized using solvothermal conditions. The networks were generated via formation of a dinuclear Eu secondary building block, involving the dicarboxylate ligand as a bridge. The luminescent properties of the Eu^{3+} complexes showed characteristic emissions at room temperature.[46]

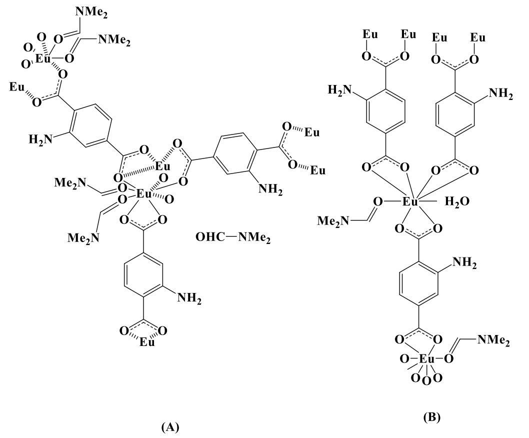

Fig. 24. Local environment of the organic linkers in A) $\{[Eu_2(NH_2BDC)_3\text{-}(DMF)_4]\cdot2DMF\}\infty$ and ,B) $Eu_2(NH_2BDC)_3(DMF)_2(H_2O)_2$

$Eu_2(NH_2BDC)_3(DMF)_2(H_2O)_2$ (Figure 24B) was prepared by reaction of Eu^{3+} with 2-amino-1,4-benzenedicarboxylic acid in presence of DMF and H_2O and their crystal structures determined by X-ray crystallography. Luminescence studies indicate 2-amino-1,4-benzenedicarboxylate ligands exhibit ineffective antenna effects, giving mainly ligand emissions at room temperature, nevertheless at 77 K, Eu-compound shows intense Eu characteristic emissions.[43]

2.5.6 *Pr-MOF*

$\{[Pr_3(NH_2BDC)_2(NH_3BDC)_4].(NO_3).8H_2O\}_n$ (Figure 25A) is a microporous MOF. It was synthesized by reaction of 2-amino-1,4-benzenedicarboxylic acid and $Pr(NO_3)_3.6H_2O$ in 2-propanol.[43] X-ray diffraction analyses reveal that its 3D structure is composed of 2-amino-1,4-benzenedicarboxylate spacers and trinuclear lanthanide nodes, in which there are two crystallographically independent lanthanide atoms, nine- and twelve-coordinated. Thermal gravimetry and powder X-ray diffraction analyses confirm that small molecules, four methanol molecules per Pr_3 unit, can be absorbed into the dehydrated microporous framework.

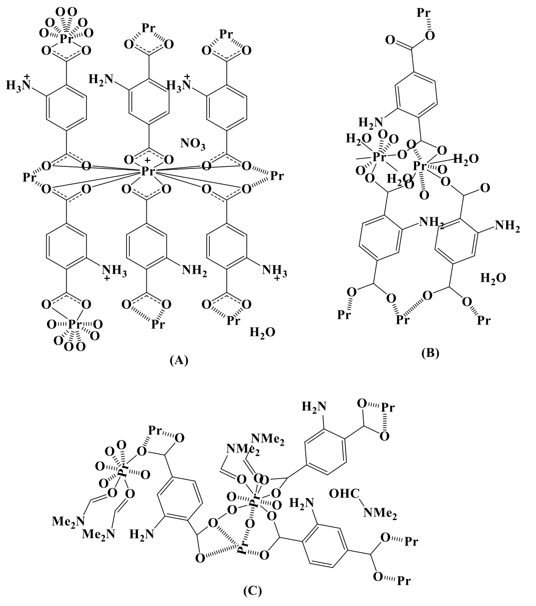

Fig. 25. Local environment of the organic linkers in A) $\{[Pr_3(NH_2BDC)_2(NH_3BDC)_4]\cdot(NO_3).8H_2O\}_n$,B)$[Pr_2(NH_2BDC)_3\cdot(H_2O)_5]\cdot 2H_2O$; C) $[Pr_2(NH_2BDC)_3(DMF)_4]_\infty$

$[Pr_2(NH_2BDC)_3\cdot(H_2O)_5]\cdot 2H_2O$, (Figure 25B) was obtained by the hydrothermal synthesis. The carboxyl groups link Pr^{3+} via the chelating or bridging bond construct 1D channels in which pendant function groups can further connect with guest water molecules in channels through hydrogen bond.[51] $[Pr_2(NH_2BDC)_3(DMF)_4]_\infty$ (Figure 25C) with cubic topology has been synthesized using solvothermal conditions and X-ray analysis show that this compound has 3D structure.[43]

2.5.6 *Gd-MOF*

The reaction of gadolinium (III) nitrate with 2-amino-1,4-benzenedicarboxylic acid in DMF at 120 ºC produces the 3D coordination network $\{[Gd_2(NH_2BDC)_3(DMF)_4]\}_n$, called MOF-LIC-1 (Figure 26A). The Gd^{3+} ions are coordinated to seven oxygen atoms belonging to five different 2-amino-1,4-benzenedicarboxylic acid ligands and two DMF molecules and exhibit a tricapped trigonal-prismatic geometry. This MOF has been modified by post-synthesis with two different functionalities and it has useful applications in the field of catalysis.[52]

$Gd_2(NH_2BDC)_3(DMF)_2(H_2O)_2$ (Figure 26B) was prepared by reaction of Gd^{3+} ions with 2-amino-1,4-benzenedicarboxylic acid in presence of DMF and H_2O and its crystal structure determined by X-ray crystallography. Each Gd atom is nine-coordinated, surrounded by one DMF, one water molecule. The Gd-compound is paramagnetic.[43]

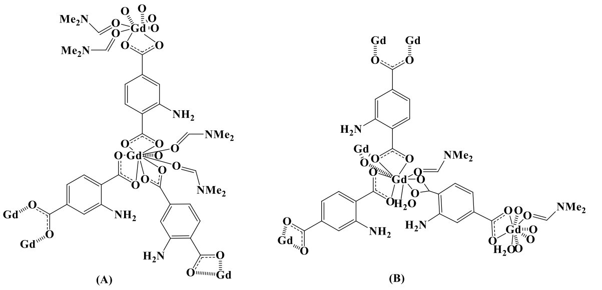

Fig. 26. Local environment of the organic linkers in A) MOF-LIC-1, B) $Gd_2(NH_2BDC)_3(DMF)_2(H_2O)_2$

2.5.7 *Sm-MOF*

$Sm_2(NH_2BDC)_3(DMF)_2(H_2O)_2$ (Figure 27) was synthesised by heating $Sm(NO_3)_3$ and 2-amino-1,4-benzenedicarboxylic acid in a 2:3 ratio in mixed DMF/H_2O solution at 80 °C. Single-crystal X-ray analysis show that this compound has a 3D framework and each Sm atom is nine-coordinated, surrounded by one DMF and one water molecule, and it has luminescent properties.[43]

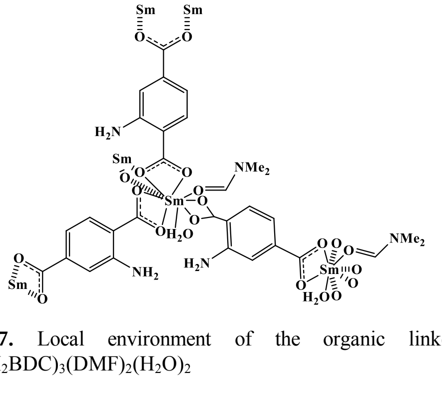

Fig. 27. Local environment of the organic linkers in $Sm_2(NH_2BDC)_3(DMF)_2(H_2O)_2$

3. Post-synthetic modification of MOFs containing 2-amino-1,4-benzenedicarboxylate.

Here I review the post-synthetic modification of MOFs. Not all synthesized MOFs with 2-amino-1,4-benzenedicarboxylic acid were modified after synthesis, but some were modified, such as IRMOF-3, DMOF-1-NH_2, UMCM-1-NH_2, MOF-LIC-1, MIL-53-NH_2, UIO-66-NH_2 and MIL-101-NH_2.

3.1. IRMOF-3

Reaction of IRMOF-3 with 1,3-propanesultone and 2-methylaziridine - IRMOF-3 reacts with 1,3-propanesultone or 2-methylaziridine in $CHCl_3$ at 45 °C to produce sulfonate and alkylamine groups via ring opening reactions (Figure 28). [53]

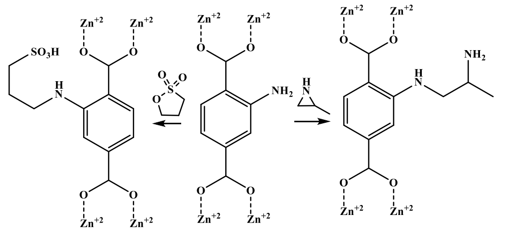

Fig. 28. Reaction of IRMOF-3 with 1,3-propanesultone and 2-methylaziridine

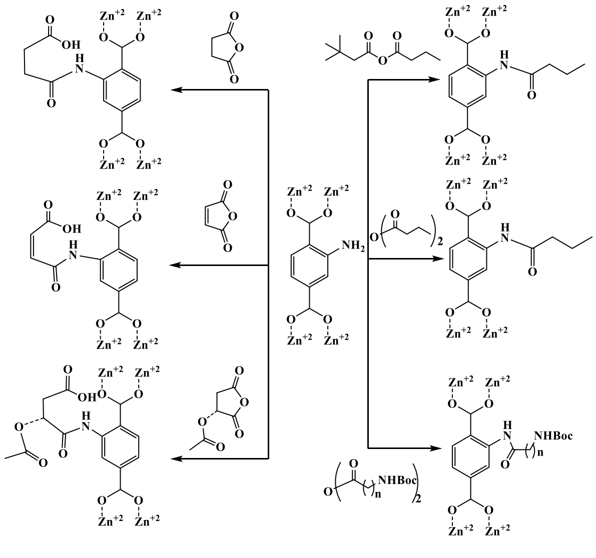

Fig. 29. Post-synthetic modification reactions performed with IRMOF-3

Reaction of IRMOF-3 with alkyl anhydride - IRMOF-3 was modified by reaction with a series of anhydrides and isocyanates. By this way, new MOF compounds with unprecedented chemical complexity were obtained (Figure 29). [54]

Reaction of IRMOF-3 with salicylaldehyde then metallation - IRMOF-3 reacted with salicylaldehyde to give salicylimine (salen). The salicylimine sites were metallated with [V(O)(acac)$_2$H$_2$O] (acac=acetylacetonate) and $NaAuCl_4$ (Figure 30). [55]

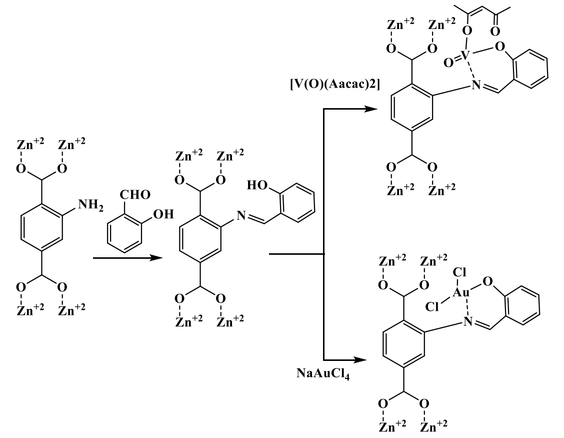

Fig. 30. Reaction of IRMOF-3 with salicylaldehyde then metallation

Reaction of IRMOF-3 with manganese (II) acetylacetonate - Bhattacharjee *et al*, [56]synthesised IRMOF-3[Mn] containing Mn(acac)$_2$ through one-step post-synthesis functionalization by binding of a manganese(II) acetylacetonate complex to IRMOF-3. The resulting MOF is a highly selective, reusable, and non-leaching catalyst for the epoxidation of several important alkenes (Figure 31).

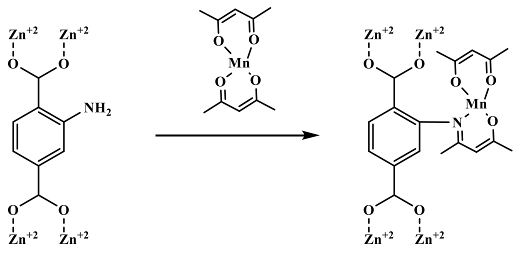

Fig. 31. Reaction of IRMOF-3 with manganese (II) acetylacetonate

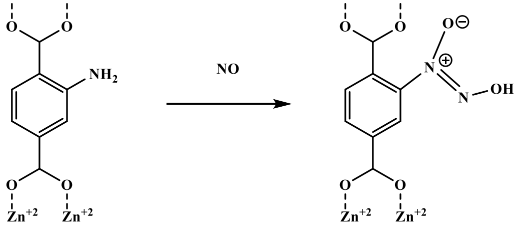

Fig. 32. Reaction of IRMOF-3 with nitric oxide

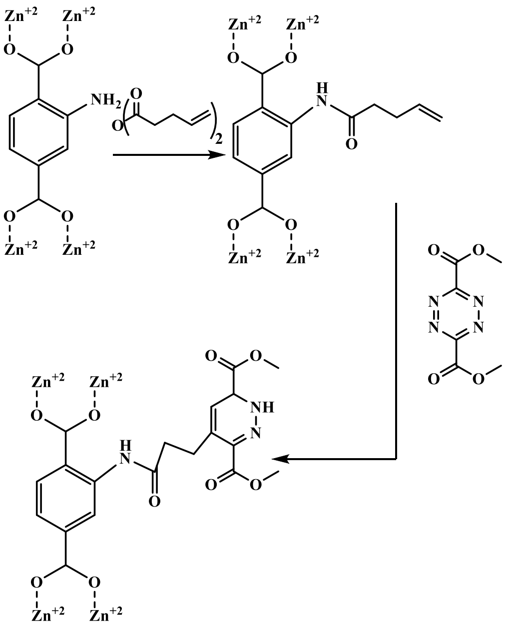

Fig. 33. Reaction of IRMOF-3 with pentenoic anhydride followed by Diels-Alder cycloaddition

Reaction of IRMOF-3 with pentenoic anhydride followed by Diels-Alder cycloaddition -Reaction of IRMOF-3 with nitrous oxide - IRMOF-3 is an excellent candidate for NO delivery and release. The amino group of IRMOF-3 react with NO at room temperature for 24 hours to yield IRMOF-3–NONO (Figure 32).[57]

IRMOF-3 was modified by reaction with pentenoic anhydride to produce IRMOF-3-(AMPent)$_n$. This material has smaller pore size and steric crowding of the olefin groups but it reacts with dimethyl-1,2,4,5-tetrazine-3,6-dicarboxylate (TDC) via Diels-Alder cycloaddition to produce dihydropyridazine MOF. The structure was confirmed by ^{1}H NMR spectra, ESI-MS analysis and single-crystal XRD. The final IRMOF-3-AMPent-TDC is highly crystalline (Figure 33). [58]

Reaction of IRMOF-3 with cyanuric chloride- IRMOF-3 was post-synthetically modified with cyanuric chloride in presence of triethylamine (Figure 34). X-ray diffraction confirms that the crystal structure of the MOF is maintained during the modification reaction and N_2 isotherms show the presence of micro- and meso-porosity in IRMOF-3 after modification.[59]

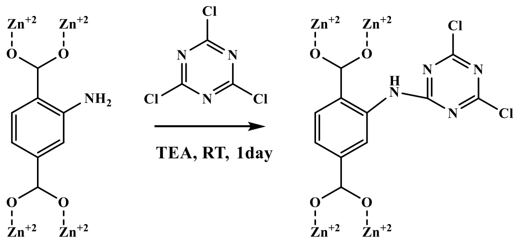

Fig. 34. Reaction of IRMOF-3 with cyanuric chloride

Post-synthetic modification of IRMOF-3 with different reagent such as ethyl oxalyl monochloride and ethyl acetoacetate (Figure 35) can offer free chelation site that can coordinate with trivalent lanthanide ions. This techniques can provide efficient near infrared (Nd^{3+}) and visible (Eu^{3+}, Tb^{3+}) light emitters.[60-63]

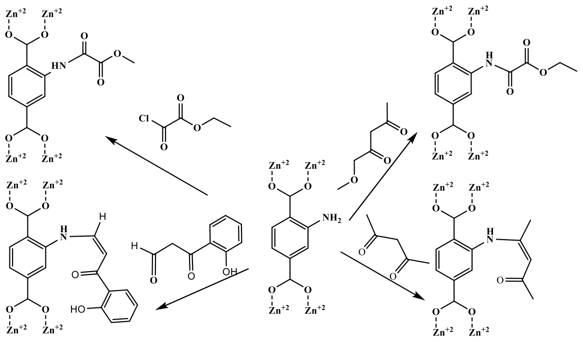

Fig. 35. Reaction of IRMOF-3 with ethyl oxalyl monochloride and ethyl acetoacetate and others

3.2. DMOF-1–NH_2

Reaction of DMOF-1–NH_2 with azide compound and cyclization (click chemistry) - The amino groups of DMOF-1–NH_2 were transformed into azides and coupled to alkynes in a one-pot reaction. The amino group of DMOF-1–NH_2 was converted into an azide using ^{t}BuONO and $TMSN_3$. The intermediate, DMOF–N3, was then treated with an excess of phenylacetylene and $Cu(CH_3CN)_4PF_6$ to generate the triazole modified DMOF, termed DMOF–fun, via 'Click' chemistry with >90% y[64]ield (Figure 36). [64]

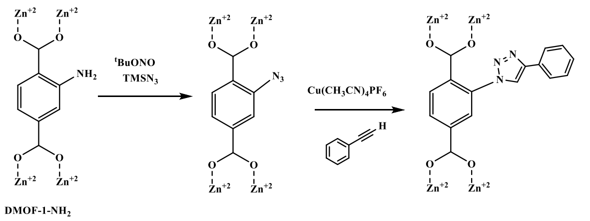

Fig. 36. Reaction of DMOF-1–NH_2 via click chemistry

3.3. UMCM-1-NH_2

Reaction of UMCM-1-NH_2 with nitric oxide- Direct modifications of UMCM-1–NH_2 is also excellent candidates for NO delivery and release. UMCM-1–NH_2 were exposed to NO at room temperature for 24 hours to yield UMCM-1–NONO (Figure 37).[57]

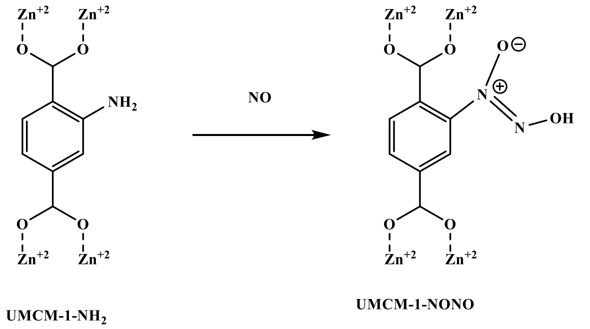

Fig. 37. Reaction of UMCM-1-NH_2 with nitric oxide

Reaction of UMCM-1-NH_2 with 2-formyl pyridine then metalation - Covalent transformation followed by metalation opens a route for incorporating metal ions into a wide range of frameworks. UMCM-1-NH_2, $(Zn_4O)_3(BDC\text{-}NH_2)_3(BTB)_4$ crystals were reacted with 2-pyridinecarboxaldehyde to form the covalently bound iminopyridine chelate derivative $(Zn_4O)_3\text{-}(BDC\text{-}C_6H_5N_2)_3(BTB)_4$, which was reacted with $PdCl_2(CH_3CN)_2$ to give the metal-complexed MOF $(Zn_4O)_3(BDC\text{-}C_6H_5N_2PdCl_2)_3\text{-}(BTB)_4$.

These reactants and products have the same structural order. UMCM-1-NH_2 has large open channels that allow for facile diffusion of reagents (Figure 38).[65]

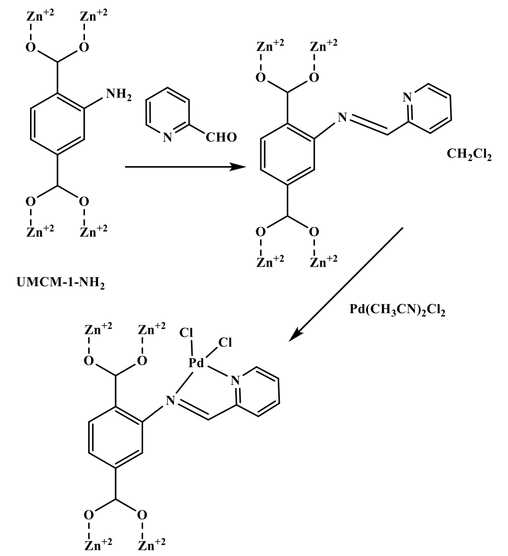

Fig. 38. Reaction of UMCM-1-NH_2 with 2-formylpyridine then metalation

Reaction of UMCM-1-NH_2 with anhydride then metallation - Post-synthetic modification may be used to introduce chelating sites into a MOF, these sites can be metallated with divalent or trivalent transition metals, and these materials can be used as catalysts for carbon–carbon bond forming reactions. UMCM-1-NH_2 was transformed with 3-hydroxyphthalic anhydride and 2,3-pyrazinedicarboxylic anhydride into UMCM-1-AMsal and UMCM-1-AMpz with percent conversions of 35% and 50%, respectively. Both modified MOFs were metallated with $Fe(acac)_3$ and $Cu(acac)_2$. The color of metallated MOFs was changed from pale yellow to dark red in the case of $Fe(acac)_3$ and in case of $Cu(acac)_2$ the color turns to bluish green. The metallated MOFs, UMCM-1–AMFesal and UMCM-1–AMCupz, were analyzed by atomic absorption (AA) analysis to quantify the metal content of the MOF. AA confirmed that UMCM-1–AMFesal contained 0.77 wt% of Fe^{3+} while UMCM-1–AMCupz had 1.76 wt% of Cu^{2+}.This materials act as a solid-state catalyst for the Mukaiyama-aldol reaction (Figure 39&40).[66]

UMCM-1-NH_2 was modified with pentenoic anhydride to produce a functionalized MOF (UMCM-1-AMPent) with an olefin group appended to the 1,4-benzenedicarboxylate ligands. UMCM-1-AMPent reacts with dimethyl-1,2,4,5-tetrazine-3,6-dicarboxylate (TDC) via Diels-Alder cycloaddition to produce dihydropyridazine MOF (UMCM-1-AMPent-TDC). The structure was confirmed by ^1H NMR spectroscopy. Single-crystal X-ray diffraction indicates that the compound is highly crystalline, stable, and microporous (Figure 39). [58]

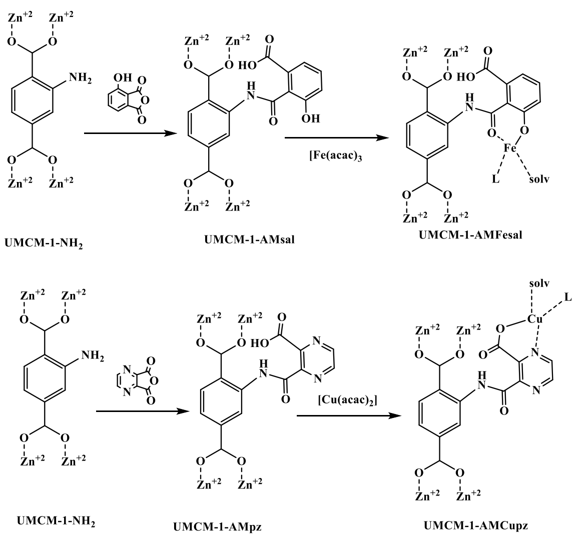

Fig. 39. Reaction of UMCM-1-NH_2 with anhydride then metallation

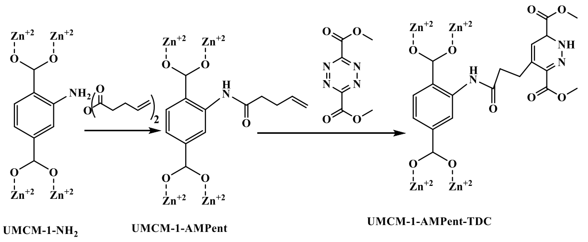

Fig. 40. UMCM-1-NH_2 was modified with pentenoic anhydride

3.4. MOF-LIC-1

Reaction of MOF-LIC-1 with ethylisocyanate, The reaction of gadolinium nitrate with 2-amino-benzene-1,4-dicarboxylic acid (NH_2BDCH_2) in DMF at 120 °C produces the 3D coordination network $\{[Gd_2(NH_2BDC)_3(DMF)_4]\}_n$ (MOF-LIC-1). MOF-LIC-1 reacts with ethylisocyanate to produce urea compound. The crystal structures of the modified MOFs demonstrate that it is possible to transform the cavities of a MOF without modifying its original 3D structure (Figure 41).[67]

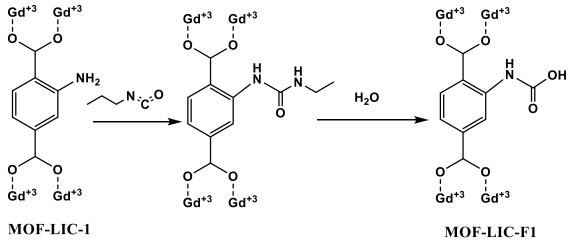

Fig. 41. Reaction of MOF-LIC-1 with ethylisocyanate

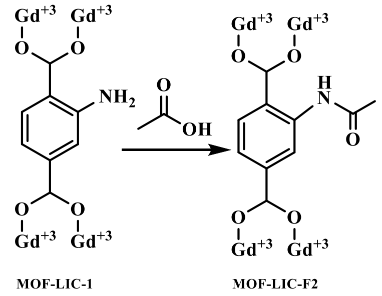

Fig. 42. Reaction of MOF-LIC-1 with acetic acid

Reaction of MOF-LIC-1 with acetic acid - MOF-LIC-1 reacts with acetic acid to produce amide function group without any change in crystalinity of MOF (Figure 42).[67]

3.5. MIL-53(Al)–NH_2

Reaction of MIL-53(Al)–NH_2 with phosgene - The free amine groups of MIL-53(Al)–NH_2 transformed into reactive iso(thio)cyanates using diphosgene or thiophosgene. MIL-53(Al)–NH_2 react with phosgene reagents to produce MIL-53(Al)–NCX (X=O or S) followed by sequential reactions with amines and alcohols to produce (thio)urea and (thio)carbamate-bearing MILs (Figure 43).[68] Reaction of MIL-53(Al)–NH_2 with alkyl anhydride - MIL-53(Al)-NH_2 was modified by treatment with acetic anhydride, succinic and maleic anhydride which results in ~40% conversion of the amine sites to products containing pendant carboxylate groups within the pores of the MOF (Figure 44).[69] Recently, MIL-53(Al)–NH_2

takes an attention in fuel purifications technology.[70] Moreover, MIL-53(Al)–NH_2 can be incorporated in cellulose acetate membrane for removal of chloropyrifos from wastewater.[71]

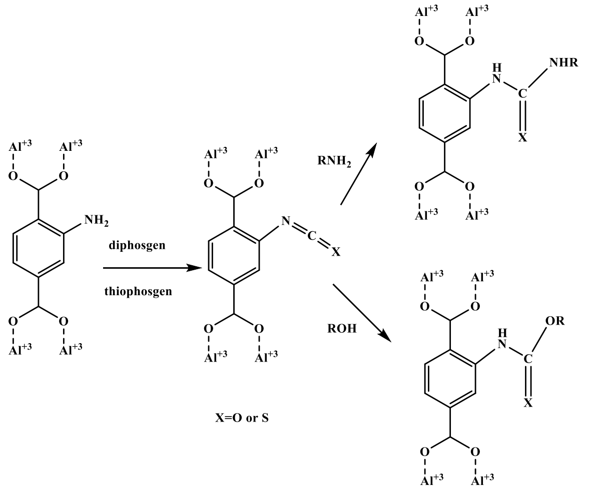

Fig. 43. Reaction of MIL-53(Al)–NH_2 with phosgene

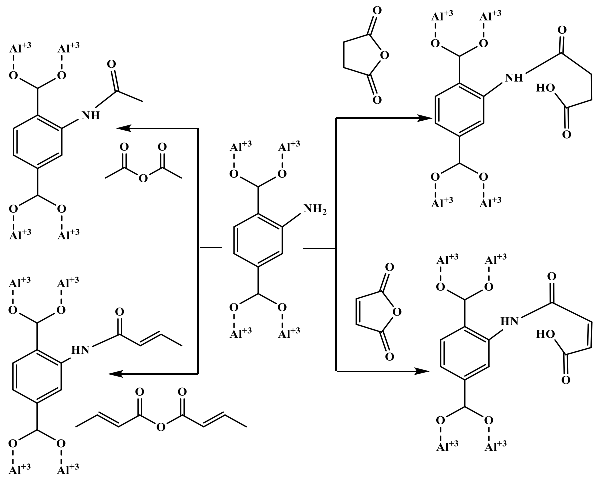

Fig. 44. Reaction of MIL-53(Al)–NH_2 with alkyl anhydrides

The presence of these Brønsted acid sites within the MOFs was exploited as an opportunity to perform heterogeneous catalysis. Indeed, the more acidic MIL-53(Al)-AMMal was found to be a good catalyst for the ring-opening reaction of epoxides with alcohols (Figure 43). [69]

3.6. UiO-66–NH_2

UiO-66 materials have very unique structures leaded to its wide range of application such as kidney dialysis application.[72] Reaction of UiO-66–NH_2 with alkyl anhydride.

The post-synthetic modification of UiO-66–NH_2 was accomplished with aliphatic and acyclic anhydrides and verified through a combination of ^1H NMR, IR, and ESI-MS analysis.

The covalent post-synthetic modification of UiO-66–NH_2 was explored using a series of alkyl anhydrides to produce amide modified frameworks designated UiO-66–AM (Figure 45).

The results show that this class of porous solid can serve as a tunable, microporous scaffold for novel applications in separations, catalysis, and biotechnology (Figure 44).[73]

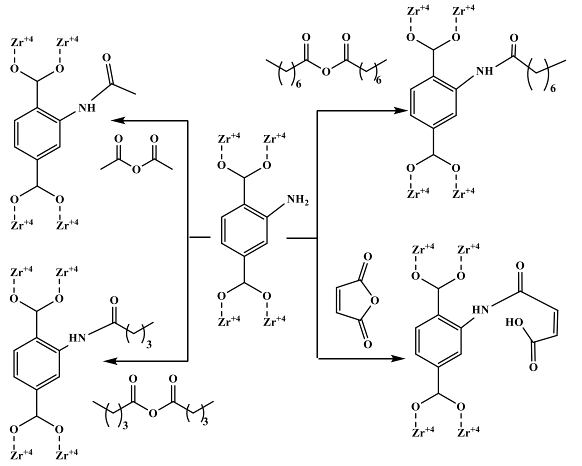

Fig. 45. Reaction of UiO-66–NH_2 with alkyl anhydrides

3.7. MIL-101–NH_2

Reaction of MIL-101–NH_2 with cisplatin - Iron-carboxylate nanoscale metal-organic frameworks was synthesized with MIL-101 structure. Very recent, MIL-101–NH_2 was used for capture of diazinon pesticide from soybean oil.[74]

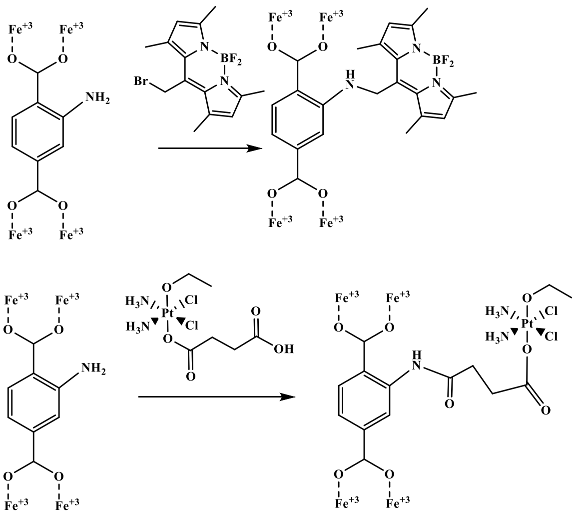

Fig. 46. Reaction of MIL-101–NH_2 with cisplatin

The presence of amino groups allows for covalent attachment of biologically relevant cargoes through post-synthetic modifications. The ethoxysuccinato-cisplatin (ESCP) prodrug,c,c,t-$PtCl_2(NH_3)_2(OEt)(O_2CCH_2CH_2CO_2H)$], was first activated by 1,1-carbonydiimidazole and then reacted with a dispersion of Iron-carboxylate NMOF in DMF at room temperature (Figure 46).

SEM imaging showed no change in the particle size or morphology after ESCP loading. This material was used for delivering high payloads of imaging contrast agents and anticancer drugs (Figure 46).[73]

3.8. MIL-125–NH_2

MIL-125–NH_2 is one of most stable MOFs that give him varieties in many application fields.[75-80] MIL-125–NH_2 was synthetically modified with dye-like molecular fragments to provide excellent photocatalytic oxidation activity under visible light irradiation.[81]

Moreover, MIL-125–NH2 was modified with chitosan for iodine uptake from wastewater (Figure 47). [82]

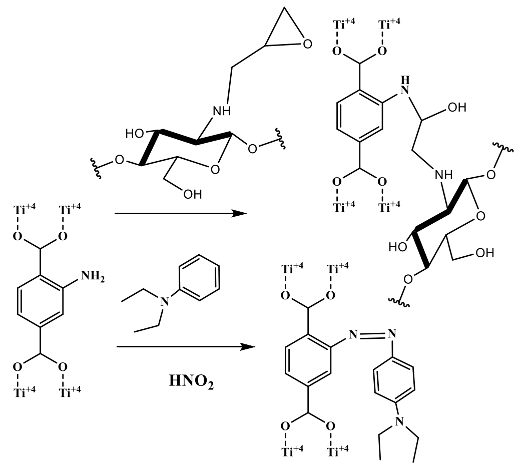

Fig. 47. Reaction of MIL-125–NH_2 with HNO_2 follows with *N, N*, diethyl aniline coupling and modified chitosan

4. Conclusion and perspective

MOFs have special properties and due to this they are promising material. The literature was growing on synthesis and applications of MOFs over the past 10 year. MOFs currently play an important role in the areas of gas storage and gas separations, catalysis and biological applications. Research on synthesis and post-synthetic modification of functional MOFs has become an important field of chemical research because it’s open new ways for the synthesis of new MOFs which cannot be prepared by old methods. The most used linker for synthesis of functionalized MOFs is 2-amino-1,4-benzenedicarboxylic acid due to it contains two carboxylic group which attached with metal and a free amino group. This amino group can be modified by reaction with organic reagent in order to produce new MOFs with new structure and new application in catalysis… etc.

5. References

[1] R. Zhao, Y. Wu, Z. Liang, L. Gao, W. Xia, Y. Zhao, R. Zou, Metal–organic frameworks for solid-state electrolytes, Energy & Environmental Science 13(8) (2020) 2386-2403.

[2] W. Fan, X. Wang, B. Xu, Y. Wang, D. Liu, M. Zhang, Y. Shang, F. Dai, L. Zhang, D. Sun, Amino-functionalized MOFs with high physicochemical stability for efficient gas storage/separation, dye adsorption and catalytic performance, Journal of Materials Chemistry A 6(47) (2018) 24486-24495.

[3] Q. Qian, P.A. Asinger, M.J. Lee, G. Han, K. Mizrahi Rodriguez, S. Lin, F.M. Benedetti, A.X. Wu, W.S. Chi, Z.P. Smith, MOF-based membranes for gas separations, Chemical Reviews 120(16) (2020) 8161-8266.

[4] J.F. Olorunyomi, S.T. Geh, R.A. Caruso, C.M. Doherty, Metal–organic frameworks for chemical sensing devices, Materials Horizons 8(9) (2021) 2387-2419.

[5] A.R.B. da Silva Galaço, K.T. de Oliveira, M.C. Donatoni, R.I. Walton, O.A. Serra, Ion-exchange resin as a new tool for characterisation of coordination compounds and MOFs by NMR spectroscopy, Chemical Communications 55(56) (2019) 8106-8109.

[6] Y. Sun, L. Zheng, Y. Yang, X. Qian, T. Fu, X. Li, Z. Yang, H. Yan, C. Cui, W. Tan, Metal–organic framework nanocarriers for drug delivery in biomedical applications, Nano-Micro Letters 12(1) (2020) 1-29.

[7] G. Boix, J. Troyano, L. Garzon-Tovar, C. Camur, N. Bermejo, A. Yazdi, J. Piella, N.G. Bastus, V.F. Puntes, I. Imaz, MOF-beads containing inorganic nanoparticles for the simultaneous removal of multiple heavy metals from water, ACS applied materials & interfaces 12(9) (2020) 10554-10562.

[8] A. Dhakshinamoorthy, Z. Li, H. Garcia, Catalysis and photocatalysis by metal organic frameworks, Chemical Society Reviews 47(22) (2018) 8134-8172.

[9] É. Whelan, F.W. Steuber, T. Gunnlaugsson, W. Schmitt, Tuning photoactive metal–organic frameworks for luminescence and photocatalytic applications, Coordination Chemistry Reviews 437 (2021) 213757.

[10] X. Li, S. Lu, D. Tu, W. Zheng, X. Chen, Luminescent lanthanide metal–organic framework nanoprobes: from fundamentals to bioapplications, Nanoscale 12(28) (2020) 15021-15035.

[11] W. Zheng, C.-S. Tsang, L.Y.S. Lee, K.-Y. Wong, Two-dimensional metal-organic framework and covalent-organic framework: synthesis and their energy-related applications, Materials Today Chemistry 12 (2019) 34-60.

[12] Y. Qin, M. Hao, D. Wang, Z. Li, Post-synthetic modifications (PSM) on metal–organic frameworks (MOFs) for visible-light-initiated photocatalysis, Dalton Transactions 50(38) (2021) 13201-13215.

[13] S. Mandal, S. Natarajan, P. Mani, A. Pankajakshan, Post-Synthetic Modification of Metal–Organic Frameworks Toward Applications, Advanced Functional Materials 31(4) (2021) 2006291.

[14] D. Kim, M.S. Lah, Metal–organic framework with two different types of rigid triscarboxylates: net topology and gas sorption behaviour, CrystEngComm 15(45) (2013) 9491-9498.

[15] M. Eddaoudi, J. Kim, N. Rosi, D. Vodak, J. Wachter, M. O'Keeffe, O.M. Yaghi, Systematic design of pore size and functionality in isoreticular MOFs and their application in methane storage, Science 295(5554) (2002) 469-472.

[16] A.L. Grzesiak, F.J. Uribe, N.W. Ockwig, O.M. Yaghi, A.J. Matzger, Polymer-induced heteronucleation for the discovery of new extended solids, Angewandte Chemie 118(16) (2006) 2615-2618.

[17] K.-L. Zhang, H.-Y. Gao, Z.-C. Pan, W. Liang, G.-W. Diao, Preparation and characterization of two three-dimensional metal–organic photoluminescent supramolecular networks, Polyhedron 26(17) (2007) 5177-5184.

[18] X.-F. Wang, Y.-B. Zhang, X.-N. Cheng, X.-M. Chen, Two microporous metal–organic frameworks with different topologies constructed from linear trinuclear M 3 (COO) n secondary building units, CrystEngComm 10(6) (2008) 753-758.

[19] K.-L. Zhang, H.-Y. Gao, N. Qiao, F. Zhou, G.-W. Diao, Preparation and characterization of two novel three-dimensional supramolecular networks with blue photoluminescence, Inorganica Chimica Acta 361(1) (2008) 153-160.

[20] Z. Wang, K.K. Tanabe, S.M. Cohen, Accessing postsynthetic modification in a series of metal-organic frameworks and the influence of framework topology on reactivity, Inorganic chemistry 48(1) (2009) 296-306.

[21] C. Quan, Y.-Q. Ren, L.-H. Xiang, L.-D. Sun, A.-E. Xu, X.-H. Gao, H.-D. Chen, X.-M. Pu, R.-N. Wu, C.-Z. Liang, Genome-wide association study for vitiligo identifies susceptibility loci at 6q27 and the MHC, Nature genetics 42(7) (2010) 614-618.

[22] X.L. Wang, C. Qin, S.X. Wu, K.Z. Shao, Y.Q. Lan, S. Wang, D.X. Zhu, Z.M. Su, E.B. Wang, Bottom-Up Synthesis of Porous Coordination Frameworks: Apical Substitution of a Pentanuclear Tetrahedral Precursor, Angewandte Chemie 121(29) (2009) 5395-5399.

[23] L.H. Wee, M.R. Lohe, N. Janssens, S. Kaskel, J.A. Martens, Fine tuning of the metal–organic framework Cu 3 (BTC) 2 HKUST-1 crystal size in the 100 nm to 5 micron range, Journal of Materials Chemistry 22(27) (2012) 13742-13746.

[24] C.-C. Shen, X.-N. Hua, L. Han, Crystal structure of poly [(4-aminopyridine-κN)(N, N-dimethylformamide-κO)(μ3-pyridine-3, 5-dicarboxylato-κ3N: O3: O5) copper (II)], Acta Crystallographica Section E: Crystallographic Communications 72(4) (2016) 440-443.

[25] Z.Y. Fu, X.T. Wu, J.C. Dai, S.M. Hu, W.X. Du, H.H. Zhang, R.Q. Sun, The Structure and Fluorescence Properties of Two Novel Mixed-Ligand Supramolecular Frameworks with Different

Structural Motifs, European Journal of Inorganic Chemistry 2002(10) (2002) 2730-2735.

[26] Y. Li, Y.-Q. Wei, L.-Z. Cai, P.-X. Li, M.-S. Wang, G.-C. Guo, Phenanthroline: A New Electron Acceptor Model for the Design and Syntheses of Photochromic Compounds, Crystal Growth & Design 19(11) (2019) 6023-6027.

[27] K.O. Kongshaug, H. Fjellvåg, Syntheses, structures and magnetic properties of Mn (II) containing 3D polymeric networks, Polyhedron 26(17) (2007) 5113-5119.

[28] X.-L. Wang, G.-D. Yang, L. Liu, A.-D. Tan, J.-C. Dai, {[Ph4P] 2 [Cd2 (tp) 2 (Htp) 2 (H2O)]· 3H2O} n and {[Ph4P][Zn (tp)(Htp)]· 2H2O} n: Two interesting 2D metal–terephthalate polymeric networks, Inorganic Chemistry Communications 48 (2014) 161-165.

[29] F.-K. Wang, S.-Y. Yang, R.-B. Huang, L.-S. Zheng, A Novel Hydrogen-Bonded 3D Network with Unusual Coordination Mode, Journal of Chemical Crystallography 40(10) (2010) 837-840.

[30] J.-J. Du, X. Zhang, X.-P. Zhou, D. Li, Robust heterometallic MOF catalysts for the cyanosilylation of aldehydes, Inorganic Chemistry Frontiers 5(11) (2018) 2772-2776.

[31] S. Bauer, C. Serre, T. Devic, P. Horcajada, J. Marrot, G. Férey, N. Stock, High-throughput assisted rationalization of the formation of metal organic frameworks in the iron (III) aminoterephthalate solvothermal system, Inorganic chemistry 47(17) (2008) 7568-7576.

[32] X.-R. Hao, X.-L. Wang, K.-Z. Shao, G.-S. Yang, Z.-M. Su, G. Yuan, Remarkable solvent-size effects in constructing novel porous 1, 3, 5-benzenetricarboxylate metal–organic frameworks, CrystEngComm 14(17) (2012) 5596-5603.

[33] H.-L. Jiang, Y. Tatsu, Z.-H. Lu, Q. Xu, Non-, micro-, and mesoporous metal− organic framework isomers: reversible transformation, fluorescence sensing, and large molecule separation, Journal of the American Chemical Society 132(16) (2010) 5586-5587.

[34] J. Chen, C.-P. Li, M. Du, Substituent effect of R-isophthalates (R=–H,–CH 3,–OCH 3,–t Bu,–OH, and–NO 2) on the construction of Cd II coordination polymers incorporating a dipyridyl tecton 2, 5-bis (3-pyridyl)-1, 3, 4-oxadiazole, CrystEngComm 13(6) (2011) 1885-1893.

[35] L. Braglia, E. Borfecchia, K. Lomachenko, A. Bugaev, A. Guda, A. Soldatov, B. Bleken, S. Øien-Ødegaard, U. Olsbye, K. Lillerud, Tuning Pt and Cu sites population inside functionalized UiO-67 MOF by controlling activation conditions, Faraday discussions 201 (2017) 265-286.

[36] P.-C. Liang, H.-K. Liu, C.-T. Yeh, C.-H. Lin, V. Zima, Supramolecular assembly of calcium metal–organic frameworks with structural transformations, Crystal growth & design 11(3) (2011) 699-708.

[37] E.C. Constable, C.E. Housecroft, 'Simple'Oligopyridine Complexes–Sources of Unexpected Structural Diversity, Australian Journal of Chemistry 73(6) (2020) 390-398.

[38] T. Ahnfeldt, N. Guillou, D. Gunzelmann, I. Margiolaki, T. Loiseau, G. Férey, J. Senker, N. Stock, [Al4 (OH) 2 (OCH3) 4 (H2N-bdc) 3]· x H2O: A 12-Connected Porous Metal–Organic Framework with an Unprecedented Aluminum-Containing Brick, Angewandte Chemie International Edition 48(28) (2009) 5163-5166.

[39] J. Gascon, U. Aktay, M.D. Hernandez-Alonso, G.P. van Klink, F. Kapteijn, Amino-based metal-organic frameworks as stable, highly active basic catalysts, Journal of Catalysis 261(1) (2009) 75-87.

[40] S. Couck, J.F. Denayer, G.V. Baron, T. Rémy, J. Gascon, F. Kapteijn, An amine-functionalized MIL-53 metal− organic framework with large separation power for CO2 and CH4, Journal of the American Chemical Society 131(18) (2009) 6326-6327.

[41] Y. Wu, N. Zheng, R. Yang, H. Xu, E. Ye, From condensed coordination structure to open-framework by modifying acid ligand, Journal of Molecular Structure 610(1-3) (2002) 181-186.

[42] C.-B. Liu, C.-Y. Sun, L.-P. Jin, S.-Z. Lu, Supramolecular architecture of new lanthanide coordination polymers of 2-aminoterephthalic acid and 1, 10-phenanthroline, New Journal of Chemistry 28(8) (2004) 1019-1026.

[43] X. Haitao, Z. Nengwu, J. Xianglin, Y. Ruyi, W. Yonggang, Y. Enyi, L. Zhengquan, Assembly of lanthanide coordination polymers with one dimensional channels, Journal of molecular structure 655(2) (2003) 339-342.

[44] H.T. Xu, N.W. Zheng, X.L. Jin, R.Y. Yang, Z.Q. Li, Channel structure of diaquasesqui (2-aminoterephthalato) dysprosium (III) dihydrate, Journal of Molecular Structure 646(1-3) (2003) 197-199.

[45] C.A. Black, J.S. Costa, W.T. Fu, C. Massera, O. Roubeau, S.J. Teat, G. Aromí, P. Gamez, J. Reedijk, 3-D lanthanide metal-organic frameworks: structure, photoluminescence, and magnetism, Inorganic chemistry 48(3) (2009) 1062-1068.

[46] J.-H. Liao, C.-S. Tsai, T.-K. Lin, Syntheses, structural characterization and luminescent properties of M2 (ATPA) 3 (DMF) 2 (H2O) 2 (M= Nd, Sm, Eu, Gd, Tb, Dy; ATPA= 2-aminoterephthalate, DMF= N, N-dimethylformamide), Inorganic Chemistry Communications 13(2) (2010) 286-289.

[47] H.T. Xu, N.W. Zheng, X.L. Jin, R.Y. Yang, Z.Q. Li, A new microporous structure constructed by a lanthanide-carboxylate coordination polymer, Journal of molecular structure 654(1-3) (2003) 183-186.

[48] J. Sienkiewicz-Gromiuk, L. Mazur, A. Bartyzel, Z. Rzączyńska, Synthesis, crystal structure, spectroscopic and thermal investigations of a novel 2D sodium (I) coordination polymer based on 2-

aminoterephthalic ligand, Journal of Inorganic and Organometallic Polymers and Materials 22(6) (2012) 1325-1331.

[49] J.-M. Zhou, W. Shi, H.-M. Li, H. Li, P. Cheng, Experimental studies and mechanism analysis of high-sensitivity luminescent sensing of pollutional small molecules and ions in Ln4O4 cluster based microporous metal–organic frameworks, The Journal of Physical Chemistry C 118(1) (2014) 416-426.

[50] Y. Luo, G. Calvez, S. Freslon, C. Daiguebonne, T. Roisnel, O. Guillou, A family of lanthanide-containing molecular open frameworks with high porosity:[Ln (abdc)(Habdc), nH2O]∞ with Ln= La–Eu and 8⩽ n⩽ 11, Inorganica Chimica Acta 368(1) (2011) 170-178.

[51] J.S. Costa, P. Gamez, C.A. Black, O. Roubeau, S.J. Teat, J. Reedijk, Chemical modification of a bridging ligand inside a metal–organic framework while maintaining the 3D structure, Wiley Online Library, 2008.

[52] D. Britt, C. Lee, F.J. Uribe-Romo, H. Furukawa, O.M. Yaghi, Ring-opening reactions within porous metal− organic frameworks, Inorganic chemistry 49(14) (2010) 6387-6389.

[53] S.J. Garibay, Z. Wang, K.K. Tanabe, S.M. Cohen, Postsynthetic modification: a versatile approach toward multifunctional metal-organic frameworks, Inorganic chemistry 48(15) (2009) 7341-7349.

[54] T. Gadzikwa, O.K. Farha, K.L. Mulfort, J.T. Hupp, S.T. Nguyen, A Zn-based, pillared paddlewheel MOF containing free carboxylic acids via covalent post-synthesis elaboration, Chemical communications (25) (2009) 3720-3722.

[55] S. Bhattacharjee, D.-A. Yang, W.-S. Ahn, A new heterogeneous catalyst for epoxidation of alkenes via one-step post-functionalization of IRMOF-3 with a manganese (II) acetylacetonate complex, Chemical Communications 47(12) (2011) 3637-3639.

[56] J.G. Nguyen, K.K. Tanabe, S.M. Cohen, Postsynthetic diazeniumdiolate formation and NO release from MOFs, CrystEngComm 12(8) (2010) 2335-2338.

[57] X.-X. Liu, S. Chen, W.-H. Fang, L. Zhang, J. Zhang, Amino-polyalcohol-solvothermal synthesis of titanium-oxo clusters: From Ti6 to Ti19 with structural diversity, Inorganic chemistry 58(11) (2019) 7267-7273.

[58] N. De, E.J. Yoo, Recent advances in the catalytic cycloaddition of 1, n-dipoles, ACS Catalysis 8(1) (2018) 48-58.

[59] M. Savonnet, D. Bazer-Bachi, N. Bats, J. Perez-Pellitero, E. Jeanneau, V. Lecocq, C. Pinel, D. Farrusseng, Generic postfunctionalization route from amino-derived metal− organic frameworks, Journal of the American Chemical Society 132(13) (2010) 4518-4519.

[60] R.M. Abdelhameed, L.D. Carlos, A.M. Silva, J. Rocha, Near-infrared emitters based on post-synthetic modified Ln 3+-IRMOF-3, Chemical Communications 49(44) (2013) 5019-5021.

[61] R.M. Abdelhameed, L.D. Carlos, A.M. Silva, J. Rocha, Engineering lanthanide-optical centres in IRMOF-3 by post-synthetic modification, New Journal of Chemistry 39(6) (2015) 4249-4258.

[62] R.M. Abdelhameed, O.M. Darwesh, J. Rocha, A.M. Silva, IRMOF-3 biological activity enhancement by post-synthetic modification, European Journal of Inorganic Chemistry (2019).

[63] R.M. Abdelhameed, D. Ananias, A.M. Silva, J. Rocha, Building Light-Emitting Metal-Organic Frameworks by Post-Synthetic Modification, ChemistrySelect 2(1) (2017) 136-139.

[64] C.J. Doonan, W. Morris, H. Furukawa, O.M. Yaghi, Isoreticular metalation of metal− organic frameworks, Journal of the American Chemical Society 131(27) (2009) 9492-9493.

[65] K.K. Tanabe, S.M. Cohen, Engineering a metal–organic framework catalyst by using postsynthetic modification, Angewandte Chemie 121(40) (2009) 7560-7563.

[66] A.D. Burrows, C.G. Frost, M.F. Mahon, C. Richardson, Post-Synthetic Modification of Tagged Metal–Organic Frameworks, Angewandte Chemie 120(44) (2008) 8610-8614.

[67] C. Volkringer, S.M. Cohen, Generating reactive MILs: isocyanate-and isothiocyanate-bearing MILs through postsynthetic modification, Angewandte Chemie 122(27) (2010) 4748-4752.

[68] S.J. Garibay, Z. Wang, S.M. Cohen, Evaluation of heterogeneous metal− organic framework organocatalysts prepared by postsynthetic Modification, Inorganic chemistry 49(17) (2010) 8086-8091.

[69] S.J. Garibay, S.M. Cohen, Isoreticular synthesis and modification of frameworks with the UiO-66 topology, Chemical communications 46(41) (2010) 7700-7702.

[70] H.E. Emam, H.B. Ahmed, H.R. El-Deib, F.M. El-Dars, R.M. Abdelhameed, Non-invasive route for desulfurization of fuel using infrared-assisted MIL-53 (Al)-NH2 containing fabric, Journal of colloid and interface science 556 (2019) 193-205.

[71] R.M. Abdelhameed, A.A. Shaltout, M.H. Mahmoud, H.E. Emam, Efficient elimination of chlorpyrifos via tailored macroporous membrane based on Al-MOF, Sustainable Materials and Technologies 29 (2021) e00326.

[72] R.M. Abdelhameed, M. Rehan, H.E. Emam, Figuration of Zr-based MOF@ cotton fabric composite for potential kidney application, Carbohydrate polymers 195 (2018) 460-467.

[73] K.M. Taylor-Pashow, J. Della Rocca, Z. Xie, S. Tran, W. Lin, Postsynthetic modifications of iron-carboxylate nanoscale metal− organic frameworks for imaging and drug delivery, Journal of the American Chemical Society 131(40) (2009) 14261-14263.

[74] R.M. Abdelhameed, M. Taha, H. Abdel-Gawad, H.E. Emam, Purification of soybean oil from diazinon insecticide by iron-based metal organic framework: Effect of geometrical shape and simulation study, Journal of Molecular Structure 1250 (2022) 131914.

[75] R.M. Abdelhameed, M. El-Shahat, H.E. Emam, Employable metal (Ag & Pd)@ MIL-125-NH2@ cellulose acetate film for visible-light driven photocatalysis for reduction of nitro-aromatics, Carbohydrate Polymers 247 (2020) 116695.

[76] R.M. Abdelhameed, H.E. Emam, Design of ZIF (Co & Zn)@ wool composite for efficient removal of pharmaceutical intermediate from wastewater, Journal of colloid and interface science 552 (2019) 494-505.

[77] H.E. Emam, R.M. Abdelhameed, Anti-UV radiation textiles designed by embracing with nano-MIL (Ti, In)–metal organic framework, ACS applied materials & interfaces 9(33) (2017) 28034-28045.

[78] H.E. Emam, H.B. Ahmed, E. Gomaa, M.H. Helal, R.M. Abdelhameed, Doping of silver vanadate and silver tungstate nanoparticles for enhancement the photocatalytic activity of MIL-125-NH2 in dye degradation, Journal of Photochemistry and Photobiology A: Chemistry 383 (2019) 111986.

[79] H.E. Emam, H.B. Ahmed, E. Gomaa, M.H. Helal, R.M. Abdelhameed, Recyclable photocatalyst composites based on Ag 3 VO 4 and Ag 2 WO 4@ MOF@ cotton for effective discoloration of dye in visible light, Cellulose (2020) 1-17.

[80] H.E. Emam, M. El-Shahat, R.M. Abdelhameed, Observable removal of pharmaceutical residues by highly porous photoactive cellulose acetate@ MIL-MOF film, Journal of Hazardous Materials 414 (2021) 125509.

[81] M.A. Nasalevich, M.G. Goesten, T.J. Savenije, F. Kapteijn, J. Gascon, Enhancing optical absorption of metal–organic frameworks for improved visible light photocatalysis, Chemical Communications 49(90) (2013) 10575-10577.

[82] M. El-Shahat, A.E. Abdelhamid, R.M. Abdelhameed, Capture of iodide from wastewater by effective adsorptive membrane synthesized from MIL-125-NH2 and cross-linked chitosan, Carbohydrate Polymers 231 (2020) 115742.